

**INVESTIGATION AND TESTING OF THE WIND TURBINE AND
PHOTOVOLTAIC SYSTEMS INTEGRATED WITH MICRO-GRID AT
UTAR CAMPUS**

NICHOLAS TEE HIENG HOCK

**A project report submitted in partial fulfilment of the
requirements for the award of Bachelor of Engineering
(Hons.) Mechatronics Engineering**

**Faculty of Engineering and Science
Universiti Tunku Abdul Rahman**

April 2013

DECLARATION

I hereby declare that this project report is based on my original work except for citations and quotations which have been duly acknowledged. I also declare that it has not been previously and concurrently submitted for any other degree or award at UTAR or other institutions.

Signature : _____

Name : _____

ID No. : _____

Date : _____

APPROVAL FOR SUBMISSION

I certify that this project report entitled **“INVESTIGATION AND TESTING OF THE WIND TURBINE AND THE PHOTOVOLTAIC SYSTEMS INTEGRATED WITH MICRO-GRID AT UTAR CAMPUS”** was prepared by **NICHOLAS TEE HIENG HOCK** has met the required standard for submission in partial fulfilment of the requirements for the award of Bachelor of Engineering (Hons.) Mechatronics Engineering at Universiti Tunku Abdul Rahman.

Approved by,

Signature : _____

Supervisor: Ir. Dr Lim Yun Seng

Date : _____

The copyright of this report belongs to the author under the terms of the copyright Act 1987 as qualified by Intellectual Property Policy of University Tunku Abdul Rahman. Due acknowledgement shall always be made of the use of any material contained in, or derived from, this report.

© 2013, Nicholas Tee Hieng Hock. All right reserved.

INVESTIGATION AND TESTING OF THE WIND TURBINE AND PHOTOVOLTAIC SYSTEMS INTEGRATED WITH MICRO-GRID AT UTAR CAMPUS

ABSTRACT

The project is about the investigation and testing of the wind turbine and photovoltaic system. The both systems were integrated with micro-grid at UTAR campus. There were two types of wind turbine covered in this project which was vertical axis wind turbine and horizontal axis wind turbine. Throughout the project, the mechanism of wind turbine and photovoltaic system had studied and investigated. These studies and investigation were conducted by review the present technologies on the related book, website, datasheet and journal for both systems. These were important to gain the background knowledge and understood the basic principle of the system at the beginning. Besides, a few different types of methodologies was conducted to investigate and test the performance of the system. Two approaches used for data collection in this project. The first approach used Power Analyzer and second approach used DAQ platform. The Power Analyzer is a ready device that used to collect data. The DAQ platform was constructed in this project and it is mainly formed by a Current Transformer, a Current Transducer, a USB chassis, a Current Card and a Voltage Card. The results had shown the accuracy of DAQ platform was better compared to Power Analyzer for data collection. The average efficiency of inverter that found in this project was about 80%.The results also indicated the performance of PV system was changing with the day time solar radiation where the performance of wind turbine was changing with the wind condition. In conclusion, the energy source of solar is more reliable compared to wind energy as the PV system is able to generate at least 5.52 kWh per day and 324.63 kWh energy per month.

TABLE OF CONTENTS

DECLARATION	ii
APPROVAL FOR SUBMISSION	iii
ABSTRACT	v
TABLE OF CONTENTS	vi
LIST OF TABLES	ix
LIST OF FIGURES	x
LIST OF SYMBOLS / ABBREVIATIONS	xiii
LIST OF APPENDICES	xv

CHAPTER

1	INTRODUCTION	16
	1.1 Overview	16
	1.2 Background and Motivation	16
	1.3 Aim of the project	18
	1.4 Objectives	18
	1.5 Contributions	19
	1.6 Organization of the Report	19
2	LITERATURE REVIEW	20
	2.1 Introduction	20
	2.2 Micro-grid	21
	2.3 Wind Turbine	21
	2.3.1 Type of Wind Turbine	21
	2.3.2 Major Components of Wind Turbine	22
	2.3.3 Wind Energy	22

2.3.4	Conversion of Mechanical to Electrical Power	23
2.3.5	Electrical Generator	24
2.3.6	Modes of Operation of Wind Turbine	25
2.4	Solar Photovoltaic	26
2.4.1	Output Power of Photovoltaic	27
2.5	Inverter	28
3	METHODOLOGY	29
3.1	Planning and Organizing	29
3.2	Research and Understanding	30
3.3	Data Collection	30
3.3.1	Method 1 - Power Analyzer	30
3.3.2	Method 2 - Data Acquisition (DAQ)	33
3.4	PV Testing	38
3.4.1	Construct of Current Transducer Platform	39
3.4.2	Power Loss along the Wires	41
3.4.3	Power Losses in the Inverter	44
3.5	HAWT Testing	47
3.6	VAWT Testing	48
3.6.1	Determine the Speed of VAWT	48
3.6.2	Test the performance of VAWT	52
4	PHOTOVOLTAIC SYSTEM	55
4.1	Overview of Photovoltaic (PV) System	55
4.2	Installation PV system	56
4.3	Construction of PV	57
4.4	Switchboard and Inverter	60
5	WIND TURBINE SYSTEM	63
5.1	Wind Turbine	63
5.1.1	Horizontal Axis Wind Turbine (HAWT) System	63
5.1.2	Vertical Axis Wind Turbine (VAWT)	71

6	RESULTS AND DISCUSSIONS	74
6.1	Comparison of Power Analyzer and DAQ platform	74
6.2	PV Output Profile	76
6.3	Power losses along the Wires in PV system	78
6.4	Power losses in the PV Inverter	80
6.5	Efficiency of PV System	83
6.6	HAWT System	84
6.7	VAWT Rotor speed	87
6.8	Performance of VAWT	88
6.8.1	Relationship between the wind and rotor speed	88
6.8.2	Relationship between the input power and output power	88
6.8.3	Relationship between rotor Speed and load	91
6.8.4	Relationship between Output Power and load	92
6.9	Overall Results	93
7	CONCLUSIONS AND RECOMMENDATIONS	94
7.1	Conclusions	94
7.2	Recommendations	95
	REFERENCES	96
	APPENDICES	98

LIST OF TABLES

TABLE	TITLE	PAGE
6.1	Results adopted from Section 3.6.1	87
6.2	Fixed Load with Variable Wind Speed	88
6.3	Fixed Wind Speed with Variable Load	91

LIST OF FIGURES

FIGURE	TITLE	PAGE
1.1	Common Type of Wind Turbine and Photovoltaic (Concinnity Solar, 2013)	18
2.1	Overview of Micro-Grid System (General Microgrids, 2012)	20
2.2	Type of Wind Turbine (a. Horizontal axis b. & c. Vertical axis) (Bracken Meyers, 2011)	22
2.3	Overview of Variable Speed Mode (Pramod, 2011)	26
2.4	Types of Photovoltaic Cell (Mukund, 2006)	26
2.5	Current versus Voltage (I-V) characteristic of the PV module (Mukund, 2006)	28
3.1	Data Collection through Power Analyzer	31
3.2	Internal Part of Control Panel	31
3.3	Wiring Connection Diagram of Power Analyzer (TES Electrical Electronic CORP, 2008)	32
3.4	Wiring Connection Diagram of DAQ platform	33
3.5	Data Collection through DAQ Platform	34
3.6	General Tab of DAQ Program User Interface	35

3.7	PV 1 Tab of DAQ Program User Interface	35
3.8	Block Diagram Developed in LabVIEW	36
3.9	Schematic Diagram of Voltage Regulator	39
3.10	Full set of Current Transducer	40
3.11	Wiring Connection Diagram of DAQ platform for Power Loss along the Wires	42
3.12	Current Transducer	42
3.13	Block Diagram of DAQ platform for Power Loss along the Wires	43
3.14	Wiring Connection Diagram for Power Losses in the Inverter	45
3.15	Block Diagram of DAQ platform for Power Loss in the Inverter	46
3.16	Wiring Connection Diagram for Rectifier	48
3.17	Testing of VAWT with Two Industrial Fan	49
3.18	Wiring Connection Diagram for VAWT Rotor Speed	50
3.19	DAQ Program User Interface for VAWT Rotor Speed	50
3.20	Block Diagram of DAQ for VAWT Rotor Speed	51
3.21	Measuring the rotor's speed of VAWT through Tachometer	51
3.22	Testing of VAWT Performance	52
3.23	50 watt (10 ohm) Variable Resistor	53
3.24	Wiring Connection Diagram for VAWT	53
3.25	Block Diagram of DAQ for VAWT Performance Test	53
4.1	Overview of PV System	55

4.2	Installation of PV Structure	56
4.3	Installation of PV System	56
4.4	PV Modules	57
4.5	PV Modules in UTAR	57
4.6	PV Switchboard	60
4.7	PV Inverter	61
4.8	Control Panel	62
4.9	Main switchboard	62
5.1	Overview of HAWT system	64
5.2	HAWT (left side is side view and right side is front view)	65
5.3	Overview of Wind Emulator System	65
5.4	Generator and Motor of Wind Emulator	66
5.5	Wind Emulator's Controller	66
5.6	Flight Controller and Inverter	67
5.7	Overview of HAWT control system	67
5.8	Interior View of Flight Controller	69
5.9	Dump Load	70
5.10	Overview of VAWT System	71
5.11	Vertical Axis Wind Turbine (VAWT)	71
5.12	Charge Controller and Battery	72
5.13	Wiring Diagram of the Controller's Terminal (TIMAR Technology Co.,Ltd)	73
6.1	Monthly Output Power Profile of PV System	77
6.2	Daily Output Power Profile of PV System	77

LIST OF SYMBOLS / ABBREVIATIONS

E	energy of PV system produced in a day, kWh
\dot{E}	kinetic energy of wind per second, Joule/s
ρ	air density, kg/m ³
ϵ	overall efficiency of power transfer from wind to generator
f	frequency of generator, Hz
i	current flow through the circuit, A
I_a	actual output current of current transformer
I_{CT}	output current of the current transformer, A
I_{max1}	PV string maximum current, A
I_{out}	output current of inverter, A
I_{pv}	output current of PV module, A
I_{SC}	PV module short circuit current, A
N_s	rotational speed of generator, rpm
P	power, W
$P_{inverter\ loss}$	power losses in the inverter, W
P_{input}	input power of the inverter, W
P_{max1}	PV string maximum power, W
P_{max}	PV module maximum power, W
P_{output}	output power of the inverter, W
P_{pv}	output power of PV module, W

$P_{wires\ loss}$	power losses along wires, W
p	number of poles per phase
R	resistance, ohm
r	radius of the rotor, m
τ	torque transferred to the rotor of generator, Nm
V_1	voltage at the start point of wires, V
V_2	voltage at the end point of wires, V
V_3	output voltage of current transducer, V
V_a	voltage of inverter's output, V
V_b	voltage of inverter's input, V
V_c	output voltage of current transducer, V
V_{drop}	voltage drop along wires, V
$V_{reg\ output}$	output voltage of voltage regulator platform, V
V_{reg}	output voltage of voltage regulator (L7805CV), V
V_{max1}	PV string maximum voltage, V
V_{min1}	PV string minimum voltage, V
V_{mp}	PV module maximum power voltage, V
V_{OC}	PV module open circuit voltage, V
V_{pv}	output voltage of PV module, V
v	speed of wind, m/s
ω	speed of generator, rad/s
φ	phase angle between voltage and current, °

LIST OF APPENDICES

APPENDIX	TITLE	PAGE
A	Gantt Chart (Semester 1)	98
B	Gantt Chart (Semester 2)	99
C	PV Inverter Datasheet A	100
D	PV Inverter Datasheet B	101
E	NI 9225 Specification A	102
F	NI 9225 Specification B	103
G	NI 9227 Specification A	104
H	NI 9227 Specification B	105
I	NI cDAQ-9174 Specification A	106
J	NI cDAQ-9174 Specification B	107
K	Photovoltaic Module Specification	108
L	HAWT Specification	109
M	VAWT Specification A	110
N	VAWT Specification B	111
O	Current Transducer Specification A	112
P	Current Transducer Specification B	113

CHAPTER 1

INTRODUCTION

1.1 Overview

An integrating of renewable energy with micro-grid at Faculty of Engineering and Sciences (FES) of University Tunku Abdul Rahman (UTAR) is presented in this project. The sources of renewable energy that had been chosen to use in this project were solar and wind energy. Hence, a photovoltaic system and a wind turbine system were used to convert the solar and wind energy into electricity. As the electricity was generated, there is a need and importance to determine the output power of the system. The performance of the system was determined through the investigation and testing on the performance of the system. The project was more towards on data collection and testing on the performance of photovoltaic and wind turbine system at UTAR campus.

1.2 Background and Motivation

The total demand of the electricity is never enough and it rises rapidly every year. In Peninsular Malaysia, the electricity has been growing between 5% and 8% every year and it could face a power shortage by 2015 based on the government's targeted growth rate of 6% per year for the next five years for the country's economy according to the commission (Leong, 2011). Hence, more power plants have to set up to overcome the rising demand of electricity. Other than the power plants, the

implementing of Feed in Tariff which had been approved by Malaysian cabinet at April 2010 also become one of the solution (Ministry of Energy, Green Technology and Water, 2011). With the implementation of Feed in Tariff, it aims to increase the generation of electricity from renewable sources of energy instead of using gas, oil, and coal to create a new demand for clean and sustainable energy sources.

Among the renewable energy, the solar and wind power had experienced remarkably rapid growth in the past 10 year. Both are pollution free sources of abundant power and eliminate the greenhouse effect which can cause by the carbon dioxide (CO₂) emitted by fossil fuel plants. The solar and wind energy are available in an endless supply compare to oil, coal and natural gas which are being rapidly depleted and becoming more expensive to extract. Meanwhile, both of them are quiet energy which means a reduction in noise pollution compare to conventional power plants. Therefore, it is suitable and encourages people to install the solar panels and wind turbines on buildings and homes to produce their own energy.

The solar and wind power have their pros and cons. The solar power is limited to the daytime solar radiation and wind power is limited to wind condition. Despite of other reason, the solar power is more suitable compare to wind power in Malaysia. The reason is due to the natural properties of Malaysia. In Malaysia, the average wind speed is low at no more than 2 m/s, non-uniformly of wind blow and its various according to region and month which have affected the output power of wind power (Ministry of Science, Technology and Innovation, 2011). Compared the wind source, the solar radiation is uniformly throughout the year as location of Malaysia is near to the equator. The common type of wind turbine and photovoltaic are shown in Figure 1.1.



Figure 1.1: Common Type of Wind Turbine and Photovoltaic (Concinnity Solar, 2013)

1.3 Aim of the project

The project is aimed to investigate and testing on the performance of the wind turbine and photovoltaic system integrated with micro-grid at Faculty of Engineering and Sciences (FES) of the University Tunku Abdul Rahman (UTAR).

1.4 Objectives

The objectives of this project are:

- To study the mechanism of the wind turbine and photovoltaic system.
- To build a platform in PC for acquiring both data from wind turbine and photovoltaic inverter.
- To show the both wind and photovoltaic power output profile.
- To identify the maximum power output of the month for wind turbine and photovoltaic system.

1.5 Contributions

The contributions involved in this project are:

- Created a platform to collect data from inverter
- Developed the LabVIEW for data collection
- Monitored the PV installation process
- Assembled and disassembled the vertical axis wind turbine
- Developed the method used to test the wind turbine and PV system

1.6 Organization of the Report

Chapter I briefly described an idea of this project. It also defines the aim, background and motivation, and objectives of the project. The literature review is written in Chapter 2. The chapter described the research, concepts, information and theory relevant on wind turbine and photovoltaic systems. The methodology of the project laid in Chapter 3. The methods and techniques used to investigate and test the performance of the systems are written in this chapter. Both system of photovoltaic and wind turbine had studied and analysed in Chapter 4 and Chapter 5. Under these chapters, several researches had done to understand the mechanism of the systems. The results and discussions are laid in Chapter 6. The results adopted from Chapter 3 were processed, analysed and discussed in this chapter. The last chapter is about to conclude the project. In this chapter, the problems encountered were listed and several recommendations for improvement on the system are proposed for further development.

CHAPTER 2

LITERATURE REVIEW

2.1 Introduction

In this project, the electricity was generated through the wind turbine (WT), solar photovoltaic (PV) and diesel generator as backup. The electricity generated was stored in the batteries and integrated with the micro-grid. The micro-grid designed in this project was operated either off-grid or on-grid. The Figure 2.1 shows the overview of micro-grid system in this project. However, it was only wind turbine and photovoltaic system will be covered in this report. Besides, there was an assumption made on this project that the power factor involved in the project will always consider as 1. Hence, all the power mentions in this project will be same value either it is true or apparent power.

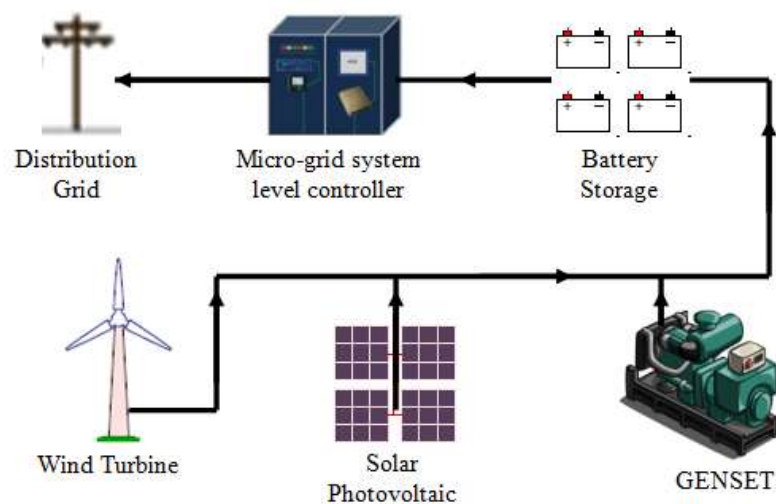


Figure 2.1: Overview of Micro-Grid System (General Microgrids, 2012)

2.2 Micro-grid

According to Remus, Marco, and Pedro (2011), a micro-grid is similar to the conventional transmission and distribution grid except the scale is much smaller. The micro-grid works by integrating all the local electricity generation and supplied to the load or grid. The electricity generation connected on micro-grid can be fuel cells, WT, PV, or any other energy sources. The micro-grid can operate in grid-connected mode or islanded mode without affects the operation of the existing grid. In this project, the micro-grid is only covered for PV and horizontal axis wind turbine.

2.3 Wind Turbine

According to Pramod (2011), a wind turbine (WT) is a device that adopts kinetic energy from wind energy into rotational form of mechanical energy and produce electricity through an electrical generator. The following subsections have discussed the basic knowledge of WT.

2.3.1 Type of Wind Turbine

According to the book written by Ahmad (2012), the wind turbine is classified based on their axis either is it horizontal and vertical. The axis is refers to their main shaft about which the rotating parts is revolve. The common type of wind turbines are horizontal axis wind turbine (HAWT) or vertical axis wind turbine (VAWT). The wind turbine is shown in Figure 2.2. The HAWT is sensitive to the direction of wind blow although in most case the wind blows horizontally while the VAWT is able to catch the wind no matter what direction of wind blow. The types of wind turbine involved in this project are vertical and horizontal axis wind turbine.

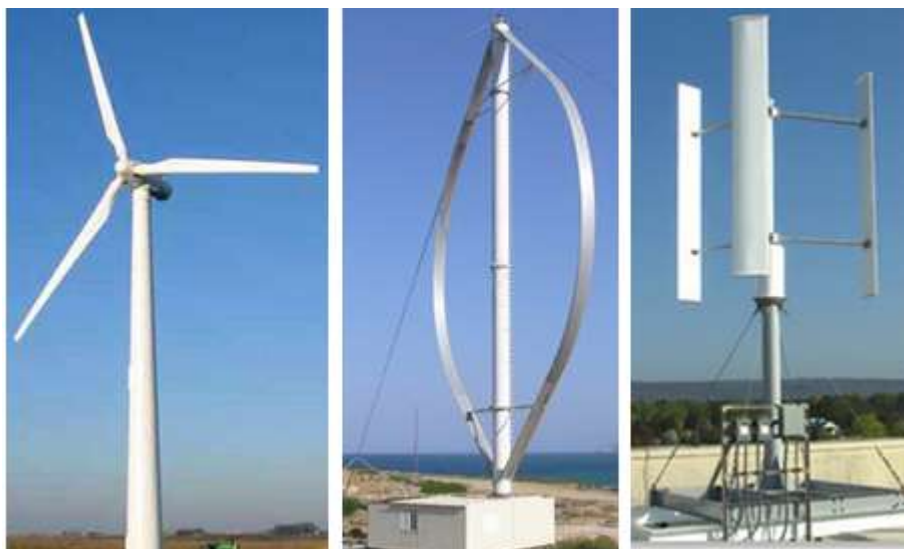


**Figure 2.2: Type of Wind Turbine (a. Horizontal axis b. & c. Vertical axis)
(Bracken Meyers, 2011)**

2.3.2 Major Components of Wind Turbine

According to the book written by Ahmad (2012), the major components for wind turbine can be classified into two parts which are mechanical and electrical components. The mechanical components are including tower, nacelle, rotor, shaft, foundation, and brake. On the other hand, the electrical component considers is only generator. All of these component are basically involved in this project either it is horizontal or vertical axis wind turbine.

2.3.3 Wind Energy

The wind energy is the prime source/energy for WT to operate as mentions in the book written by author Pramod (2011). The energy adopted from the wind is type of linear kinetic energy and it can be expressed in equation 2.1.

From the equation 2.1, it is obtained that the kinetic energy of wind power is affected by the speed, air density and the rotor of wind turbine. Hence, it is possible to increase the wind power by increases the size of rotor although the speed and air density of wind are variable with the weather condition.

$$\dot{E} = \frac{1}{2} \rho \pi r^2 v^3 \quad (2.1)$$

where

\dot{E} = kinetic energy of wind per second, Joule/s

v = speed of wind, m/s

ρ = air density, kg/m³

r = radius of the rotor, m

2.3.4 Conversion of Mechanical to Electrical Power

As the prime energy is defined, the linear kinetic energy is then converted into the rotational kinetic energy through the blade and shaft either with gearbox or directly. According to Pramod (2011), the mechanical power can be expressed in equation 2.2 and the electrical power is expressed in equation 2.3

$$\tau \omega = \epsilon \dot{E} \quad (2.2)$$

where

ω = speed of generator, rad/s

ϵ = overall efficiency of power transfer from wind to generator

\dot{E} = kinetic energy of wind per second, Joule/s

τ = torque transferred to the rotor of generator, Nm

$$\tau\omega = Vi \cos \varphi \quad (2.3)$$

where

ω = speed of generator, rad/s

τ = torque transferred to the rotor of generator, Nm

V = AC voltage, V

i = current flow through the circuit, A

φ = phase angle between voltage and current, °

From the above equation, it is obtained that the current and phase angle are depend on the amount of torque supply to the rotor of generator by assuming both voltage and angular frequency are constant. However, the torque is depends on the kinetic energy from the wind. As a result, the current and phase angle is still depending on the wind condition.

2.3.5 Electrical Generator

The electrical generator is a machine used to generate electricity from the mechanical source of energy. In the book written by Ahmad (2012), the generator used by wind turbine is Alternative Current (AC) generator and it is commonly the generator is 3 phase synchronous.

According to the Pramod (2011), the frequency of the generator is relying on the generator rotor speed. The frequency of the synchronous generator can be expressed as shown in equation 2.4.

Based on the equation 2.4, is it obtained that the lower the number of pairs of poles per phase, the faster the generator must be rotated in order to have same frequency. Due to the fact that all the poles in synchronous generator must accommodated in a circular area that forms the stator of the generator, the size and

structure of the generator is depends on the number of poles. Therefore, a generator with more poles will generally has a bigger size and shorter in length.

$$N_s = \frac{120 \times f}{p} \quad (2.4)$$

where

f = frequency of generator, Hz

p = number of poles per phase

N_s = rotational speed of generator, rpm

2.3.6 Modes of Operation of Wind Turbine

Mode of operation is explained as the way a WT connected to a grid as stated by the author Pramod (2011). The modes of operation available for synchronous generator are direct drive mode, fixed speed mode and variable speed mode.

In variable speed mode, the turbine is connected to the generator through the same shaft without a gear box between them. This mode is able to change the speed of rotor such that the turbine is operating at peak power for all wind speeds will yield higher energy output. The overview of variable speed mode is shown in Figure 2.3. The principle of variable speed mode stated by the author is written in next paragraph.

In the Figure 2.3, the speed of generator is controlled by a pulse width modulated (PWM) type of inverter. The control mechanism is works such a manner that optimal values of current from rectifier are drawn by the inverter. These optimal values of current determine the current flows through the stator coils which also determine the optimal value of torque and angular velocity of the generator. Therefore, the speed of rotor is increased by reduced the current drawn by the

inverter and the speed of rotor is reduced by increased the current drawn by the inverter. In addition, the variable speed mode is able to deliver reactive power to the grid. The amount of reactive power is controlled by using an inductor and controlling the inverter output voltage and its phase angle relative to the grid.

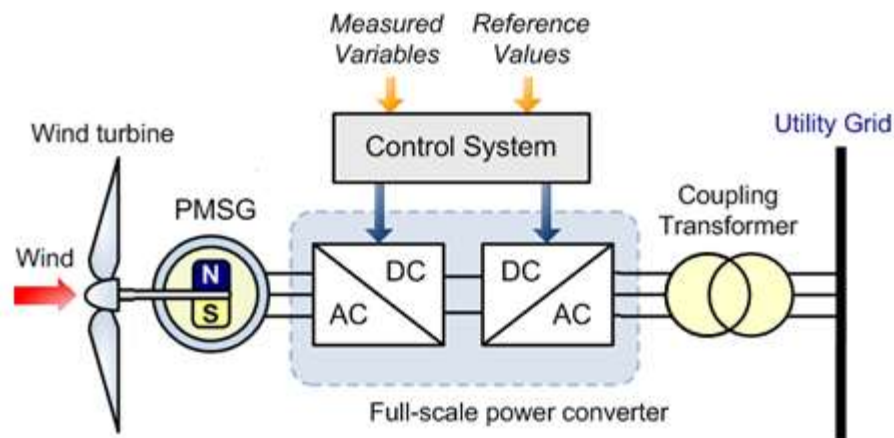


Figure 2.3: Overview of Variable Speed Mode (Pramod, 2011)

2.4 Solar Photovoltaic

By referring to the book written by Mukund (2006), the solar photovoltaic is a semiconductor device that uses the photovoltaic effect to generate DC electricity directly from the sun radiation. The principle behind the direct use of the sun's energy for the production of electricity was discovered in 1887 by Heinrich Hertz and explained in 1905 by Albert Einstein.

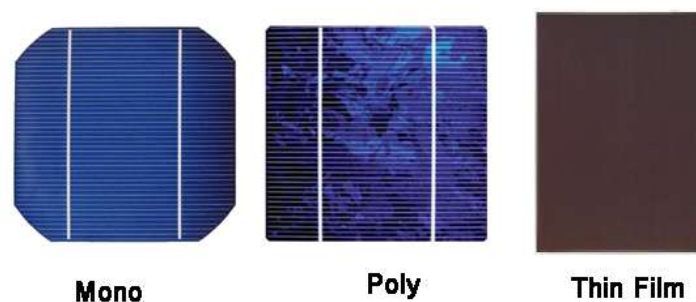


Figure 2.4: Types of Photovoltaic Cell (Mukund, 2006)

The major types of solar photovoltaic are monocrystalline silicon, polycrystalline silicon and thin film. The conversion efficiency of the monocrystalline is the highest among other. The difference of solar photovoltaic can be obtained by their surface's colour as shown in Figure 2.4.

2.4.1 Output Power of Photovoltaic

According to the book written by Mukund (2006), the output power of a photovoltaic module is direct current and it can be determined from the equation

$$P_{pv} = I_{pv} \times V_{pv} \quad (2.5)$$

where

P_{pv} = output power of PV module, W

V_{pv} = output voltage of PV module, V

I_{pv} = output current of PV module, A

From the equation 2.5, it is obtained that the output power is depends on the voltage and current output. The output power is equal to zero if either one of the value voltage or current is zero. The maximum power is adopted when the voltage and current has the maximum current. However, this is not true based on the Current and Voltage characteristic of PV module as shown in Figure 2.5.

Based on the Figure 2.5, the PV module is works as a constant current source and generating a voltage to match with the load resistance. Until a certain level of voltage, the current is drops rapidly with a small rise in the voltage to supply the internal resistance. Therefore, it is necessary to vary the voltage in range of 0 to V_{mp} in order to adopt the maximum output power.

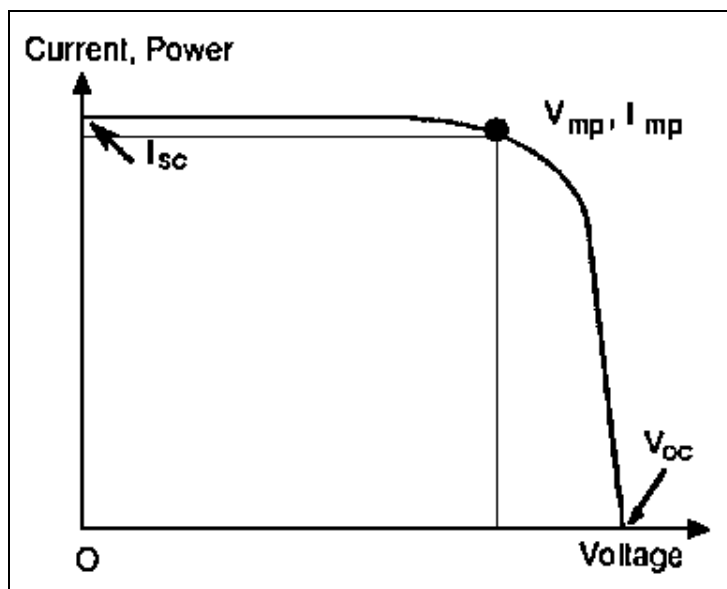


Figure 2.5: Current versus Voltage (I-V) characteristic of the PV module (Mukund, 2006)

In addition, the author also explains that the output power is directly affected by the sun intensity or amount of solar radiation (W/m^2). The amount of solar radiation and the angle sun shine direct hits on the surface of PV module are affected the current and output power of the PV module. During the sunny day, the solar radiation is high, more current is flows inside the PV module and the output power is higher compare to a cloudy day.

2.5 Inverter

According to the Remus, Marco, and Pedro (2011), the inverter is a devices used to interface the DC power source into the grid system. Typically, the functions of an inverter are tracking the maximum power point, anti-islanding, grid synchronization and data logger instead of inverting DC power only. The types of inverter included module integrated inverters, string inverters, multistring inverters, mini central inverters and central inverters. However, there is only string inverters are covered in this project. The string inverter has their own inverter for each string or multi string unit to invert the DC power.

CHAPTER 3

METHODOLOGY

3.1 Planning and Organizing

The project started from the May 2012 and ended at April 2013. The duration for this project is two semesters. The overall planning and organizing of the project are shown in Appendix A and Appendix B.

During the first semester, the progress was planned quite slowly due to construction of the wind turbine and photovoltaic systems were not yet completed. Hence, more time had used to study and review the system implemented by other. In the first semester, the data collection, researches, investigation and testing were focused on photovoltaic system.

The studies and researches of wind turbine had conducted in second semester. The system of wind turbine were researched, tested and investigated in second semester. At the end of semester, the time was used on the report writing and analysing the results.

3.2 Research and Understanding

In the previous chapter, it was known the project was more towards to data collection and analysis of the data. In the meantime, the performances of the systems were also been investigated and tested in this project. In order to ensure the investigation and testing on the system can be safely been performed, the research was first implemented on the systems. These research and understanding will allows the task to be performs without damage the equipment and devices. Besides, it also helps on analyses the results obtained.

All the researches were conducted by studying articles, journals, books and manufacture datasheet to get more ideas and information. The detail's researches of photovoltaic and wind turbine system are written in Chapter 4 and Chapter 5.

3.3 Data Collection

This section will discuss on the methodology used to collect the data from output of inverter. The data collected were the information of voltage and current from the output of inverter. Based on Chapter 4 and Chapter 5, the inverters used for wind turbine and photovoltaic system were similar where both outputs were in alternative current (AC) form. Hence, the method used for data collection could be the same type. In this project, two methods were used to collect the data from inverter.

3.3.1 Method 1 - Power Analyzer

The equipment power analyzer (model TES - 3600) was used to collect the data in first method. This power analyzer is capable to sense the voltage and current in AC form and store the data based on the setting set up. The data was collected by power analysed as shown in Figure 3.1 and Figure 3.2. It is always keep in mind to switch off the PV source and disconnects the grid system with the inverter before any

further progress. If fail to do so, it may damages the devices or electric shock may happens as the electrical power involved is high.

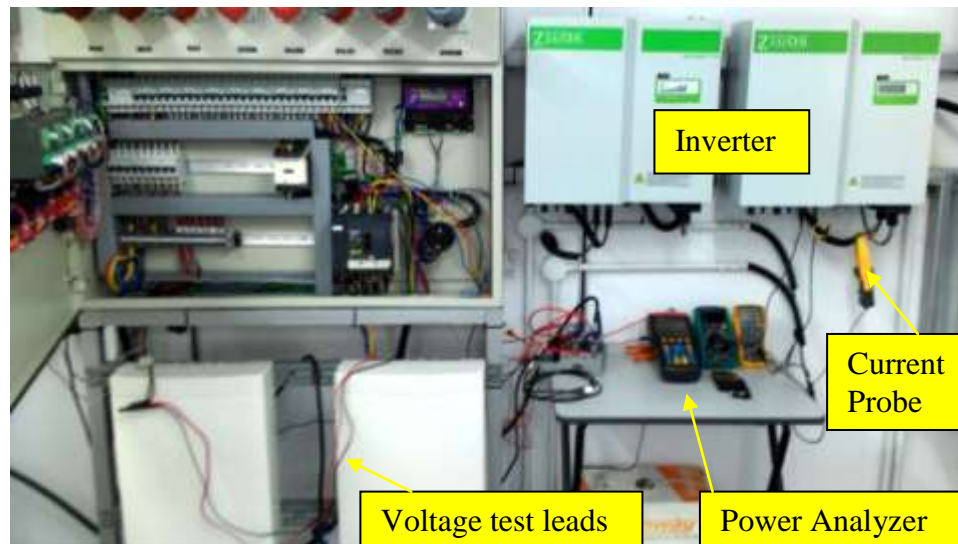


Figure 3.1: Data Collection through Power Analyzer

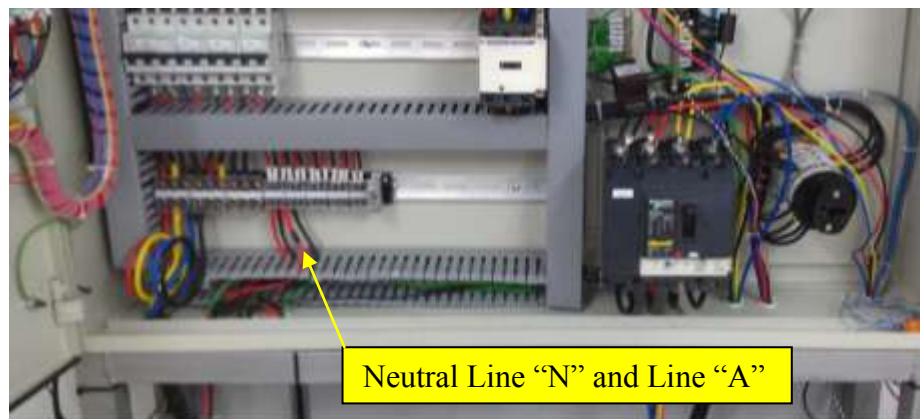


Figure 3.2: Internal Part of Control Panel

In these figure, the current probe (used to sense current) was clamped on the line wire (red colour) while the two voltage test leads (used to sense voltage) was connected to the line wire (red colour) and neutral wire (black colour). Both current probe and voltage test leads were then connecting back to power analyzer to sense and store the data in memory.

The detail of wiring diagram for power analyzer and inverter is shown in Figure 3.3. In this figure, it had clearly shown the black and red voltage test leads were connected to terminal “U1” and “1”. The current probe output plug was connected to the terminal “I1”.

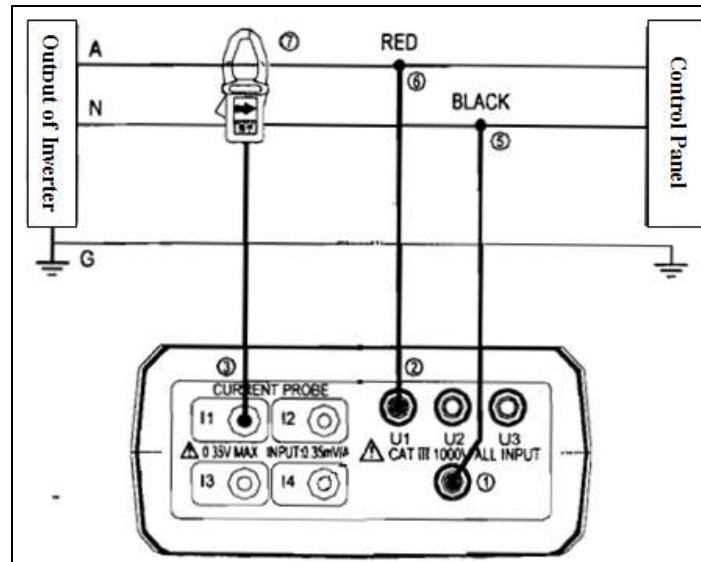


Figure 3.3: Wiring Connection Diagram of Power Analyzer (TES Electrical Electronic CORP, 2008)

As the full wiring connection had done, the timing for power analyzer was calibrated and it was set to store the data each second throughout the day. Then, the switch for PV was switched on and feeds to the grid system. The data stored was transferred to computer every two days as the memory size of power analyzer is limited. The transfer process had done through the RS 232 interface.

The data transferred to the computer was saved and further been processed through the program Microsoft Excel. These results are then analysed and discussed in Chapter 6.

3.3.2 Method 2 - Data Acquisition (DAQ)

The second method for data collection had done through the data acquisition (DAQ) platform. The DAQ platform was formed by a voltage card (model NI 9225), a current card (model NI 9227) and an USB chassis (NI cDAQ-9174). The voltage card was used to measure output voltage while the current was measured by current card. Both voltage and current card were slotted in USB chassis to communicate with computer through the program developed in LabVIEW.

Based on the Chapter 4 and 5, the output of inverters was in AC form. Based on the manufacture's datasheet as shown in appendix D, the nominal output voltage was 230 V and 13 A for nominal output current. On the other hand, the measurement range for voltage card is $-300 V_{\text{rms}}$ to $+300 V_{\text{rms}}$ and $-5 A_{\text{rms}}$ to $+5 A_{\text{rms}}$ measurement range for current card are shown in appendix E to H. Hence, it was not possible to measure the inverter's output current directly as it may spoil the current card. The problem was solved by adding a current transformer (ratio 250:5 A) to step down the output current to range of current card before connects to the current card.

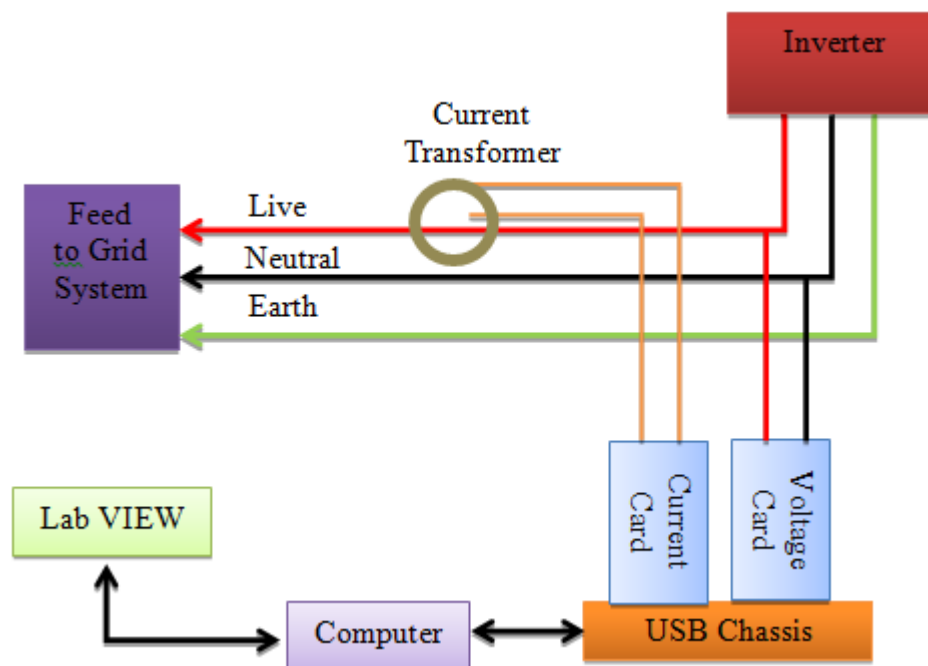


Figure 3.4: Wiring Connection Diagram of DAQ platform

The wiring connection diagram for DAQ platform with the inverter is shown in Figure 3.4. In the figure, the current transformer was hooked at the live wires to sense the current and the output of current transformer was connected to the current card. The output voltage was sensed by voltage card through the direct parallel connection. Both cards were slotted into the USB chassis and connected to computer through USB cable.

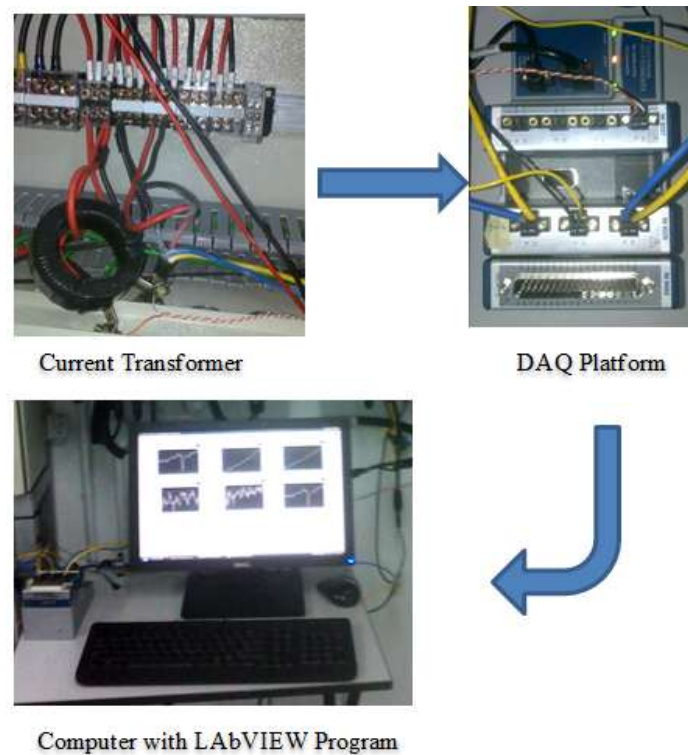


Figure 3.5: Data Collection through DAQ Platform

In the computer, a program was developed in LabVIEW to display and store the data. The actual connection is shown in Figure 3.5. All the wiring connection had done when the PV source and grid system were disconnected from inverter.

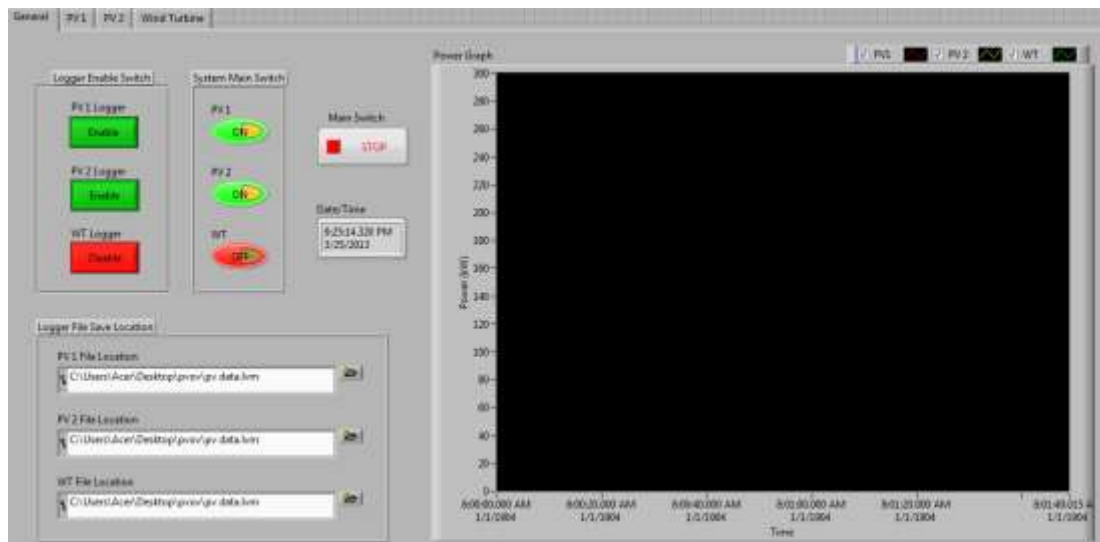


Figure 3.6: General Tab of DAQ Program User Interface

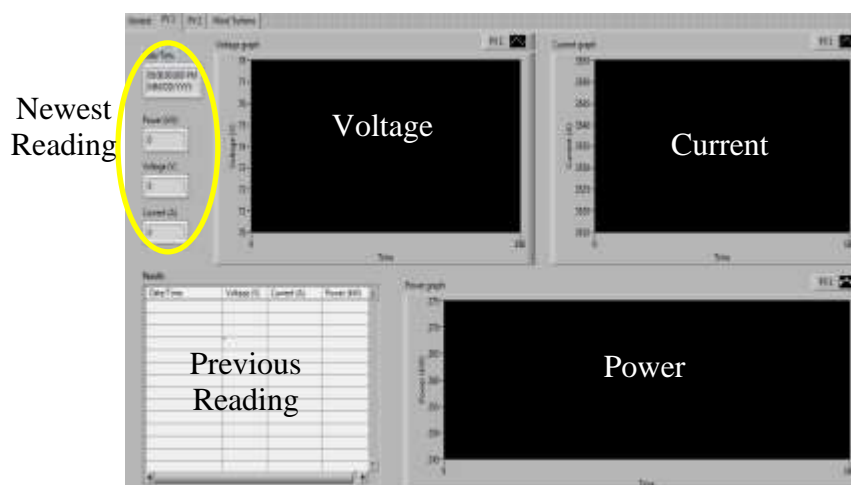


Figure 3.7: PV 1 Tab of DAQ Program User Interface

The developed DAQ program user interface in LabVIEW is shown in Figure 3.6 and Figure 3.7. This program was developed to collect data from three inverters (PV 1, PV 2 and wind turbine) either single operating or simultaneously. In the Figure 3.6, four tabs were created to display different data and uses. The “general” tab was created as control and summary display purpose. It allows user to control the program main switches, switches to adopt each inverter’s data, switches for each logger for data storage and setting for data to be save. The graph in “general” tab was used to shown the power (kW) against time for three set of inverter’s data.

The user interfaces for other three tabs are basically same to each other. The only different was the data was collected from different set of inverter. The tab “WT” is shown the wind turbine output profile while tab “PV1” and tab “PV2” are shown the photovoltaic output profile from the inverters. These three tabs were indicated the voltage (V), current (A) and power (kW) from the inverter. It’s indicated present’s reading and previous reading in the result table. The three graphs display in each tabs were indicated the voltage (V), current (A) and power (kW) versus time.

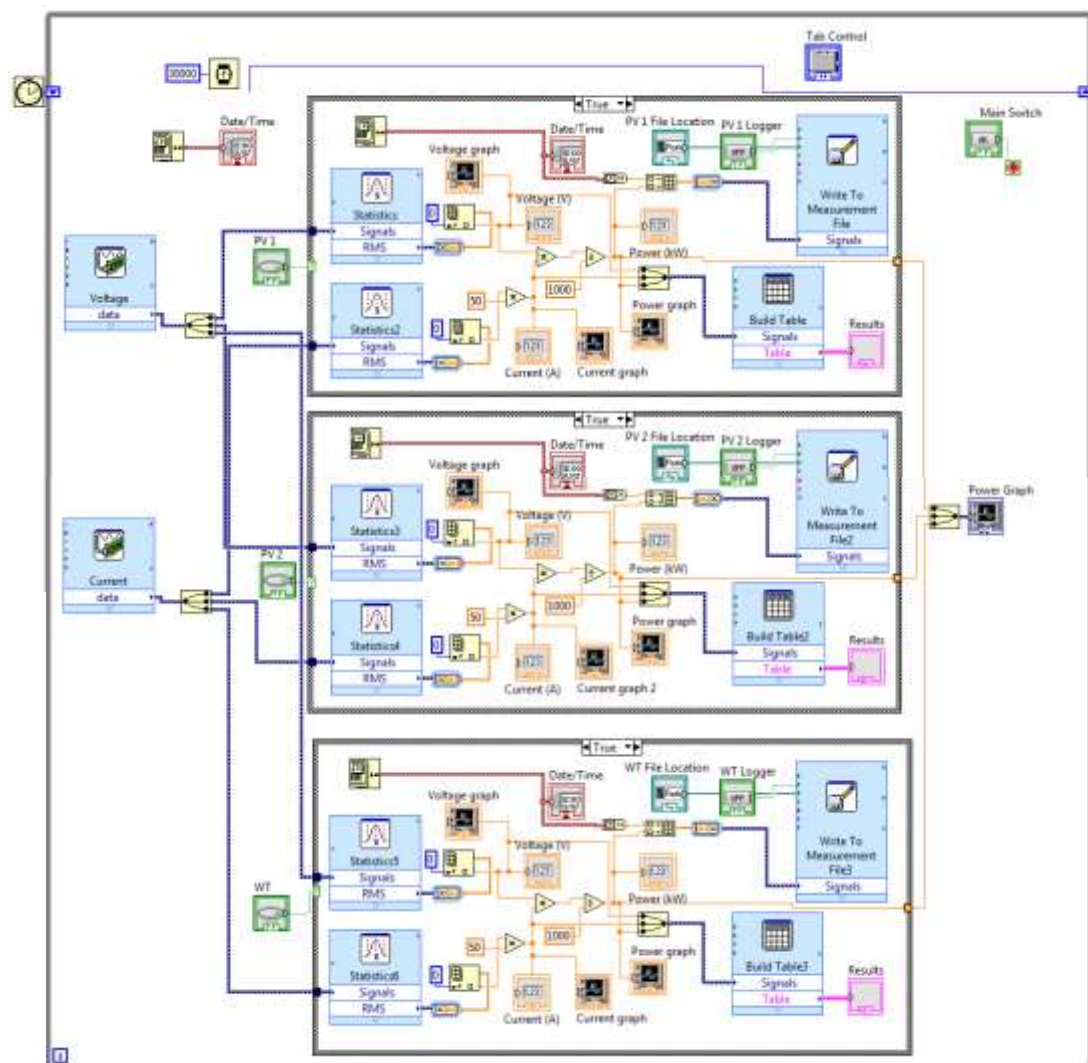


Figure 3.8: Block Diagram Developed in LabVIEW

The block diagram used for DAQ program user interface was developed in LABVIEW as shown in the Figure 3.8. The block diagram is quite complicated as a lot of wiring are involved. However, the main function was to adopt and the data was stored for every 30 seconds. Before storing the data, the data was calibrated and calculated to get the final value. For example, the current transformer was calibrated to the actual value as shown in equation 3.1. The inverter's output power (kW) was calculated based on equation 2.5.

$$\begin{aligned}
 I_{out} &= CT \text{ ratio} \times I_{CT} \\
 &= \frac{250}{5} \times I_{CT} \\
 &= 50 \times I_{CT}
 \end{aligned}
 \tag{3.1}$$

where

I_{out} = output current of inverter, A

I_{CT} = Output Current of the Current Transformer, A

$CT \text{ ratio}$ = ratio of current transformer

The data stored in computer were processed in program Microsoft Excel. These data were merged, recalculated to get the average data and categorised with the date. Then, the graph of power (kW) versus time (hour) was plotted and the output profile of month was created. These outcomes are further been shown and discussed in Chapter 6.

3.4 PV Testing

This section is about the methodology used to test the performance of photovoltaic system. Under this section, the power losses along the photovoltaic system were investigated and tested. The power losses in photovoltaic system were including the losses along the wires and the losses inside inverter during power conversion.

Based on the joule's law, the power dissipated in a resistor is in term of the current flow through it and its resistance. It was known that the joule law can be applied to any circuit that is obeys ohm's law. Therefore, both equation of ohm's law and joule's law can be combined as shown in equation 3.2.

$$P = I^2 \times R \quad (3.2)$$

where

P = power , W

R = resistance, ohm

I = current, A

The power losses in the PV system can be found by determine the values of voltage, current or resistance along the system based on the equation 2.5 and 3.2. The information of voltage (V) and current (A) were more reliable compared to resistance. This is because the resistance may change as it was affected by temperature and conductivity. Therefore, power losses in the PV system were determined in term of voltage and current.

From the Chapter 4, the output power from photovoltaic was in direct current (DC) form while the maximum output current was 16.84 A and maximum output voltage was 296 V. The current transformer used in previous section was unable to sense DC current as it only work for AC current. At the same time, the current card (model NI 9227) also not suitable as the current involved was out of the measurement range. Hence, an additional current transducer platform was constructed in this section to sense the DC current.

3.4.1 Construct of Current Transducer Platform

The Hall Effect current transducer (model CSL2DC) was selected to sense current in this project. This type of current transducer had advantages to sense current in either AC or DC form and most important the cost is low. The output of this current transducer was voltage signal and it was open loop linear type. Hence, the output voltage signal was proportional to the measured primary current. However, the requirement of stable power supply to power up current transducer was its main drawback.

Based on the manufacture datasheet as shown in appendix O and P, the supply voltage required was 8 to 12 Volts. Besides, it was understood that the current transducer was sensitive to the voltage supplied. Due to this issue, the voltage regulator was constructed to provide a steady voltage for this current transducer.

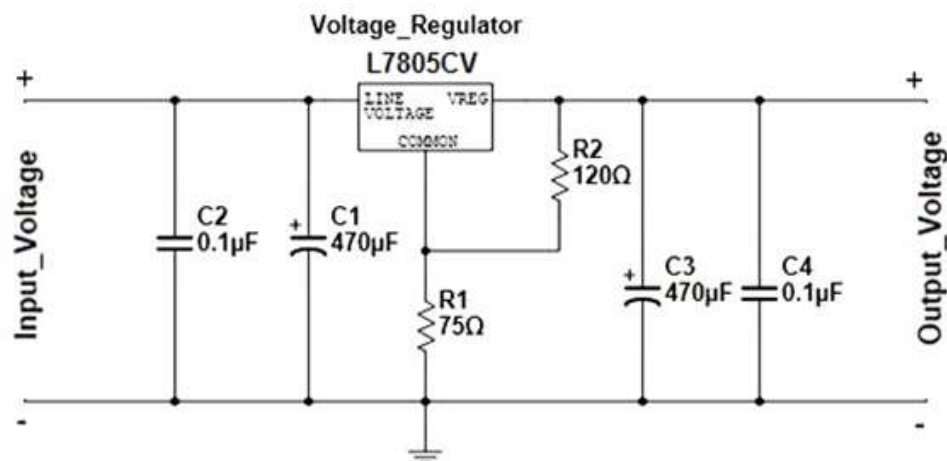


Figure 3.9: Schematic Diagram of Voltage Regulator

The circuit diagram of voltage regulator is shown in Figure 3.9. The voltage regulator were designed to output 8V (DC voltage) with input of 12 V (DC voltage). In Figure 3.9, the input was supplied by a 12 V DC wall adaptor and the output voltage was connected to current transducer. The 5V voltage regulator (L7805CV) with resistors ($R1 = 75\text{ohm}$ and $R2 = 120\text{ohm}$) were used to convert from 12 V into 8 V. The calculation for voltage regulator is shown in equation 3.3.

$$\begin{aligned}
 V_{reg\ output} &= V_{reg} \times \left(\frac{R_1 + R_2}{R_2} \right) \\
 &= 5 \times \left(\frac{75 + 120}{120} \right) \\
 &= 8.125\ V
 \end{aligned}
 \tag{3.3}$$

where

$V_{reg\ output}$ = output voltage of voltage regulator platform, V

V_{reg} = output voltage of voltage regulator (L7805CV), V

R_1 = 75 ohm resistor

R_2 = 120 ohm resistor

The monolithic ceramic capacitors (C2 and C4) were placed parallel on each side of voltage regulator to reduce the ripple voltage amplitude and filter out any noise. While, the electrolytic capacitors (C1 and C3) help the regulator deals with surges in power and smooth the ripple voltage amplitude.

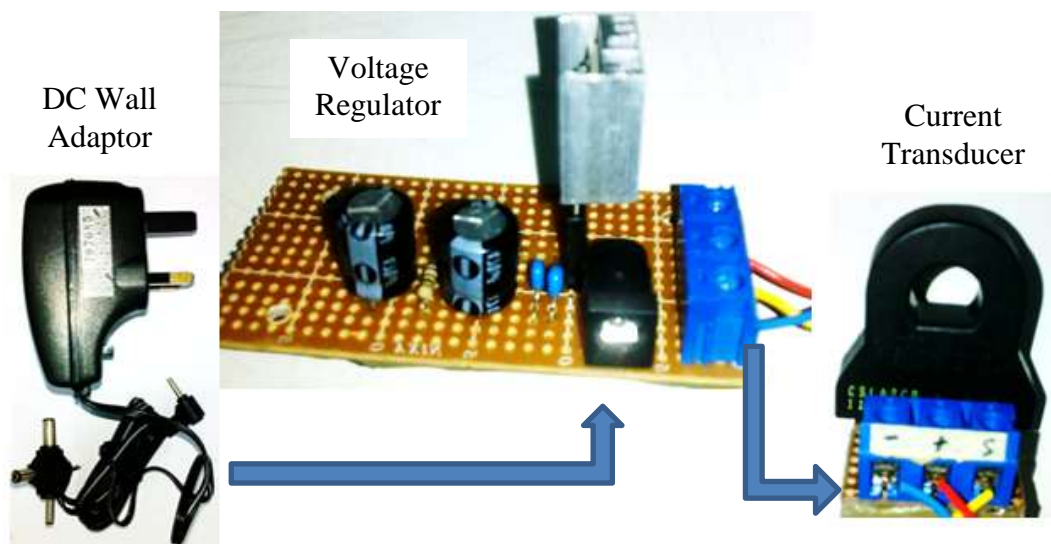


Figure 3.10: Full set of Current Transducer

The complete set of current transducer platform was built and shown in Figure 3.10. The current transducer and voltage regulator were linked through wires instead of built on the same board. Although, all the components were built in the same board which can save some the cost and size. However, it was not flexible in this project as the current transducer was required to hook on the wire for long period to measure the current and it will be quite heavy if all the components were built in a same board.

3.4.2 Power Loss along the Wires

The power losses in the wires were referred to the wires starts from output of PV switchboard to the input of inverter. The total length of the wires along the PV system was measured by using measuring tape and it is about 57 meter. The power losses along the wires were determined by measures current, I_{pv} and the voltage, V_{drop} along the wires as shown in the equation 3.4.

$$P_{wires\ loss} = I_{pv} \times V_{drop} \quad (3.4)$$

where

$P_{wires\ loss}$ = power losses along wires, W

I_{pv} = output current of PV modules, A

V_{drop} = voltage drop along wires, V

The DAQ method was used in this section to collect the data. The main equipment involved were current transducer platform constructed in previous section, voltage card (model NI 9225) and an USB chassis (NI cDAQ-9174). The wiring diagram is shown in Figure 3.11. Based the Figure 3.11, the voltage (V_1 and V_2) were measured by parallel connection between voltage card and the terminal. The current transducer was hooked on the wire as shown in figure 3.12 and output a

voltage signal, V_3 . The voltage V_3 was measured by connecting to the voltage card. Then, a program was developed in LabVIEW to store the data.

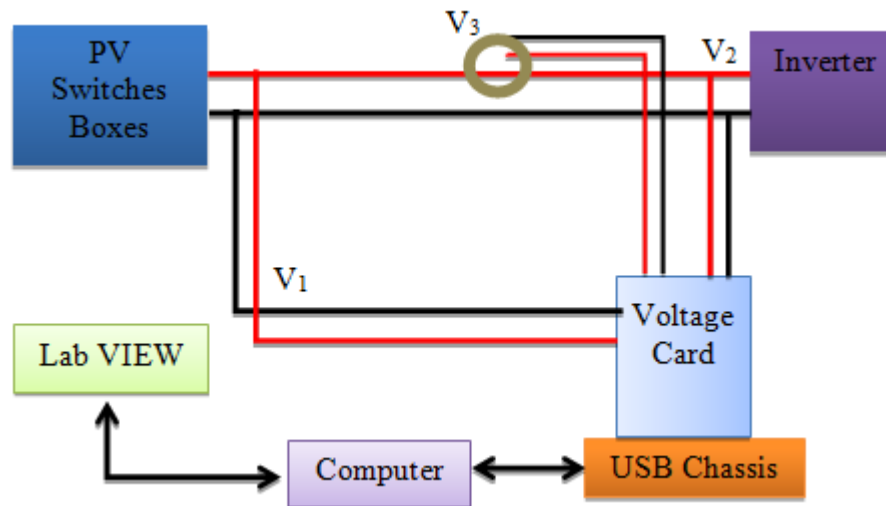


Figure 3.11: Wiring Connection Diagram of DAQ platform for Power Loss along the Wires



Figure 3.12: Current Transducer

The block diagram developed in LabVIEW is shown in Figure 3.13. All the wiring connection was done when the PV source and grid system were disconnected from the inverter. In the Figure 3.13, the block diagram was designed to adopt the data from chassis, store the data for each second and performs some calculation to get the final value before it was stored.

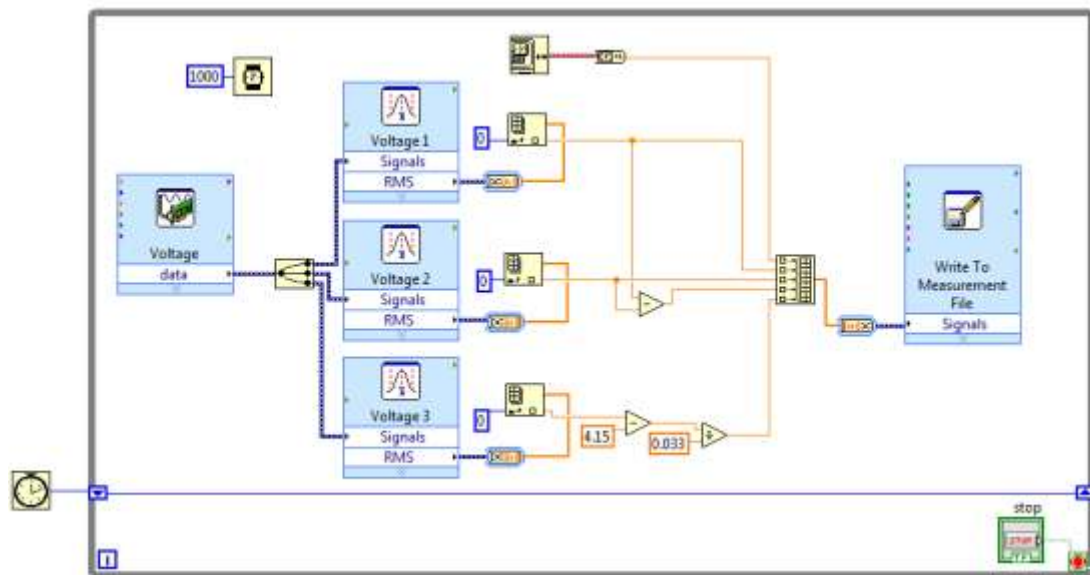


Figure 3.13: Block Diagram of DAQ platform for Power Loss along the Wires

The calculations involved in the block diagram were the calibration for current transducer, I_{pv} and voltage drop along the wires, V_{drop} . The calibration for current transducer was based on the resolution provided by manufacture datasheet and it was expressed in equation 3.5. Meantime, the calculation for V_{drop} is shown in equation 3.6.

$$I_{pv} = \left(\frac{V_3 - \left(\frac{V_{reg\ output}}{2} \right)}{0.033} \right) \quad (3.5)$$

where

I_{pv} = output current of PV modules, A

V_3 = output voltage of current transducer, V

$V_{reg\ output}$ = output voltage of voltage regulator platform, V

$$V_{drop} = (V_1 - V_2) \quad (3.6)$$

where

V_{drop} = voltage drop along wires, V

V_1 = voltage at the start point of wires, V

V_2 = voltage at the end point of wires, V

By having these values, the power losses along the wires were calculated in Microsoft Excel and graph of V_{drop} versus I_{pv} was plotted. These results are shown in Chapter 6.

3.4.3 Power Losses in the Inverter

The power losses in the inverter can be determined by measures the input power and output power of the inverter. The difference between the input power and output power of the inverter will be the power losses in the inverter. The power losses in the inverter was expressed as

$$P_{inverter\ loss} = P_{input} - P_{output} \quad (3.7)$$

where

$P_{inverter\ loss}$ = power losses in the inverter, W

P_{input} = input power of the inverter, W

P_{output} = output power of the inverter, W

These input and output power of the inverter were determined by helps of current transducer platform, current transformer, voltage card (model NI 9225), a current card (model NI 9227) and an USB chassis (NI cDAQ-9174). The method used was DAQ method which was similar as previous sections.

The output power was determined same way as Section 3.3.2 and the wiring connection diagram is shown in Figure 3.4. While, the determination of input power was similar to Section 3.4.2 but it was slightly simpler as only one voltage signal was measured. The complete wiring connection diagram is shown in Figure 3.14 and the block diagram is shown in Figure 3.15.

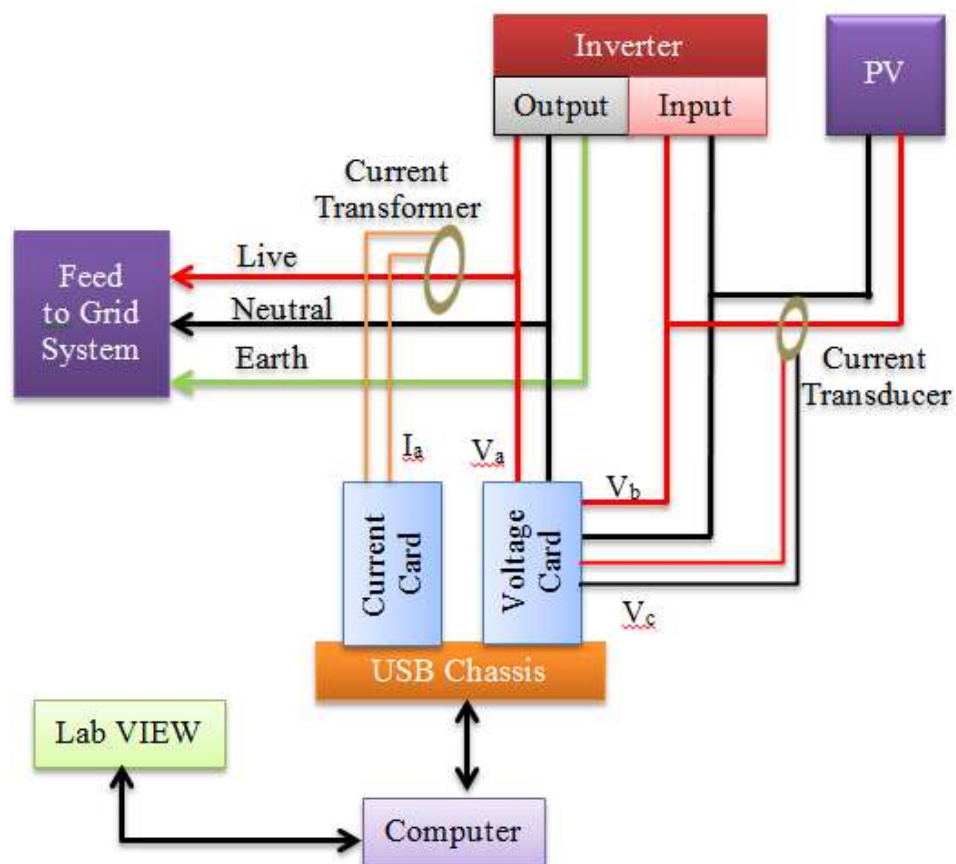


Figure 3.14: Wiring Connection Diagram for Power Losses in the Inverter

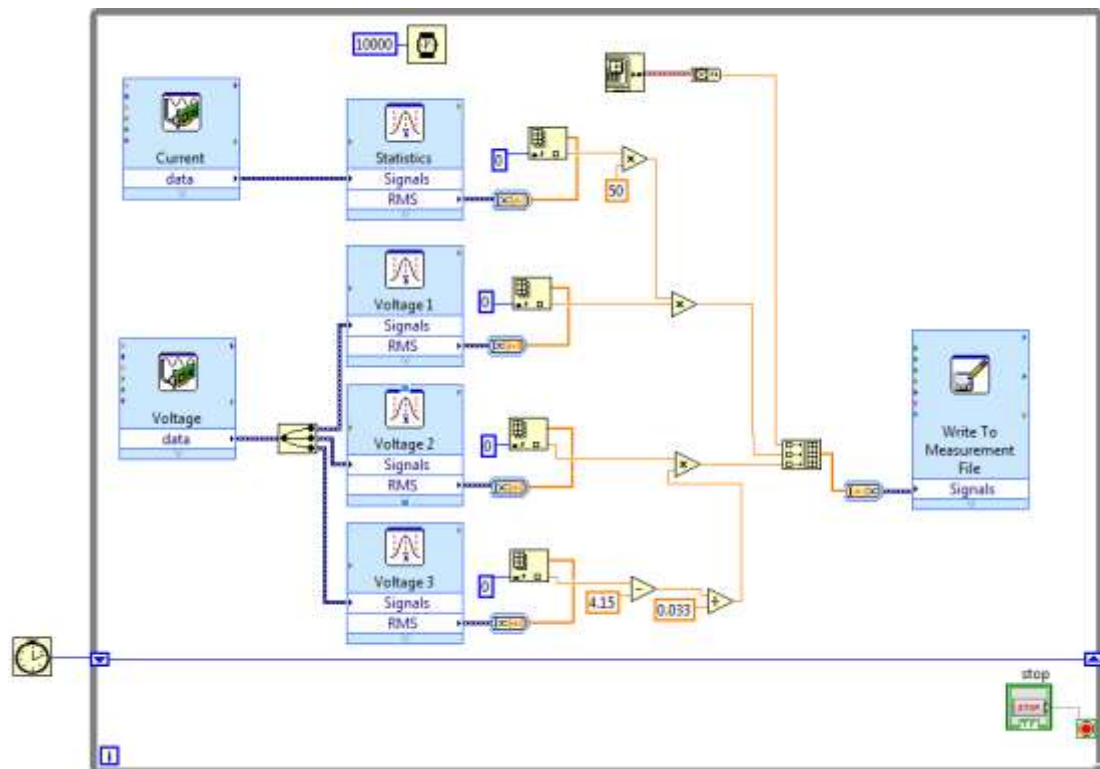


Figure 3.15: Block Diagram of DAQ platform for Power Loss in the Inverter

In the Figure 3.15, the power of inverter was adopted and stored for every 10 seconds. The calibrations for input and output power of inverter used in block diagram were shown in the equation 3.8 and 3.9.

$$P_{input} = \left(\frac{V_c - \left(\frac{V_{reg\ output}}{2} \right)}{0.033} \right) \times V_b \quad (3.8)$$

where

P_{input} = input power of inverter, W

V_b = voltage of inverter's input, V

V_c = output voltage of current transducer, V

$V_{reg\ output}$ = output voltage of voltage regulator platform, V

$$P_{output} = 50 \times I_a \times V_a \quad (3.9)$$

where

P_{output} = output power of inverter, W

I_a = actual output current of current transformer, A

V_a = voltage of inverter's output, V

These data were processed in program Microsoft Excel to find the power losses and efficiency of the inverter. The graph of efficiency versus input power was plotted as shown in Chapter 6.

3.5 HAWT Testing

This section is about the methodology used to investigate and test the performance of HAWT system. Based on the Chapter 5, the wind turbine was generating the 3 phase AC form power and it was converted into the single phase DC form power before feed to the inverter. The performance of inverter was excluded in this section as it was similar with the performance of PV inverter as done in Section 3.4.3. Hence, the performance converter was much interest to be covered in this section.

The converter of these AC to DC power had done by three phase to single phase full bridge rectifier as shown Chapter 5. The test was performed on this rectifier to test the efficiency of the power conversion. It is only input and output voltage will be measured as the electrical power was unable to determine due to the malfunction of inverter.

The methodology used for this section was simple and it had done by manually measure of voltage through conventional multimeter. The wiring connection diagram is shown in Figure 3.16. In the Figure 3.16, the AC input source of rectifier was come from the wind emulator than wind turbine. This is to ensure the

input voltage was always constant at all the time. The AC input voltage source was balanced so the line voltage can be measured within any two wires out of the three wires. As mention in the Chapter 5, the circuit for generator was in star connection where the line voltage was equal to $\sqrt{3}$ multiply phase voltage. Then, calculation had done to find the AC phase voltage. The input and output voltage of rectifier were measured with different level of speed. The speed was increased slowly from 0 to 400 rpm. The results were recorded and processed in program Microsoft Excel as shown in chapter 6.

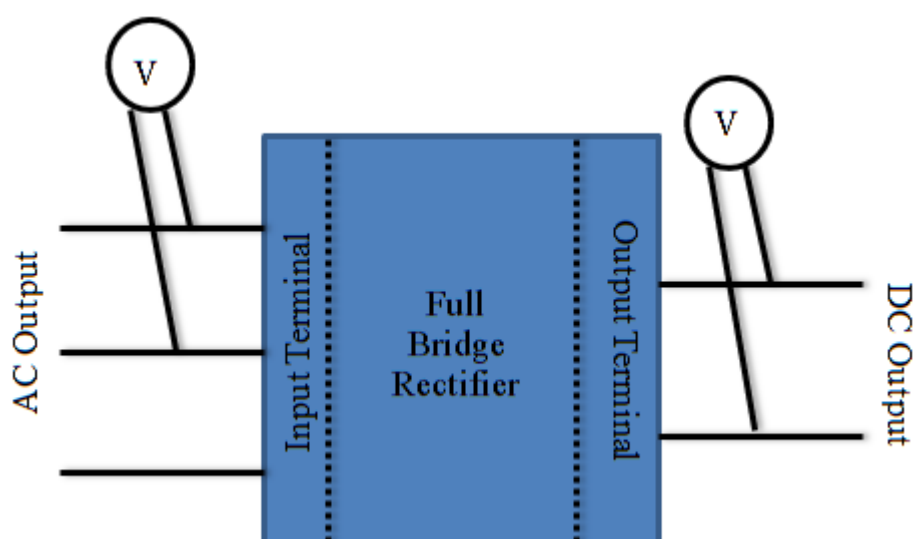


Figure 3.16: Wiring Connection Diagram for Rectifier

3.6 VAWT Testing

3.6.1 Determine the Speed of VAWT

The speed of VAWT was determined in this section instead of the wind speed. The reason was the cost of equipment used to test the wind speed was high compare to the equipment used for speed test. Hence, the information of VAWT's speed was used to define the relationship between the wind speed and output power.

The speed mention here was about the speed of VAWT rotates or named as rotor's speed. The speed was measured in term of radius per minute (rpm). For example, one rpm simply means the VAWT is rotates about a full 360 degree circle in a minute. Based on the Chapter 5, the rotor was rotated together with the synchronous generator. Therefore, the equation 2.4 in Chapter 2 can be used to determine the rotor speed.

From the equation 2.4, the number of poles per phase and frequency of generated EMF were both unknown. Hence, the both information were required to determine before determine the speed of rotor. The frequency of generated EMF was actually same as the voltage's frequency generated by the generator. The frequency for voltage can be adopted through the DAQ methods. The number of poles per phase can be determined through experiment and DAQ methods.



Figure 3.17: Testing of VAWT with Two Industrial Fan

The equipment used for this section were two industrial fan, a voltage card (model NI 9225), an USB chassis (NI cDAQ-9174), and a tachometer (model DT-2236). The industrial fans were used to simulant the wind stream for VAWT to rotate

constantly as shown in Figure 3.17. The experiment was done at in door to avoid the natural wind act on the rotor speed. The height of both industrial fans was adjusted to be same height with the centre of VAWT rotor. The distance between VAWT and fans were arranged to be same. The wiring connection diagram is shown in Figure 3.18. It is only two wires were required to connect to the voltage card as the output of VAWT were balanced.

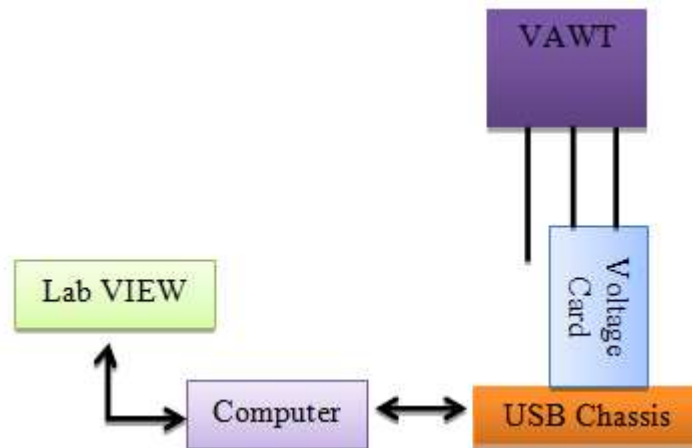


Figure 3.18: Wiring Connection Diagram for VAWT Rotor Speed

The user interface and block diagram of DAQ platform were constructed in program LabVIEW as shown in Figure 3.19 and Figure 3.20. The block diagram was simply as it only adopts frequency of voltage and equation 2.4 was inserted to find the rotor speed. The user interface was only used to adjust the number of poles, indicates the rotor speed and frequency of voltage.

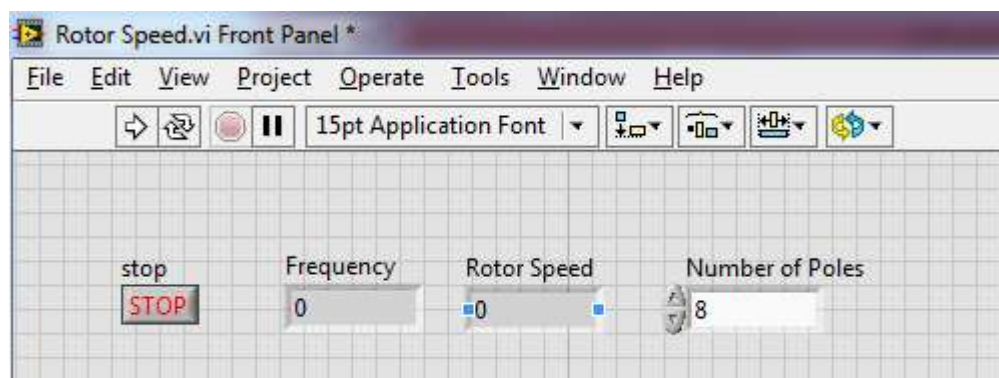


Figure 3.19: DAQ Program User Interface for VAWT Rotor Speed

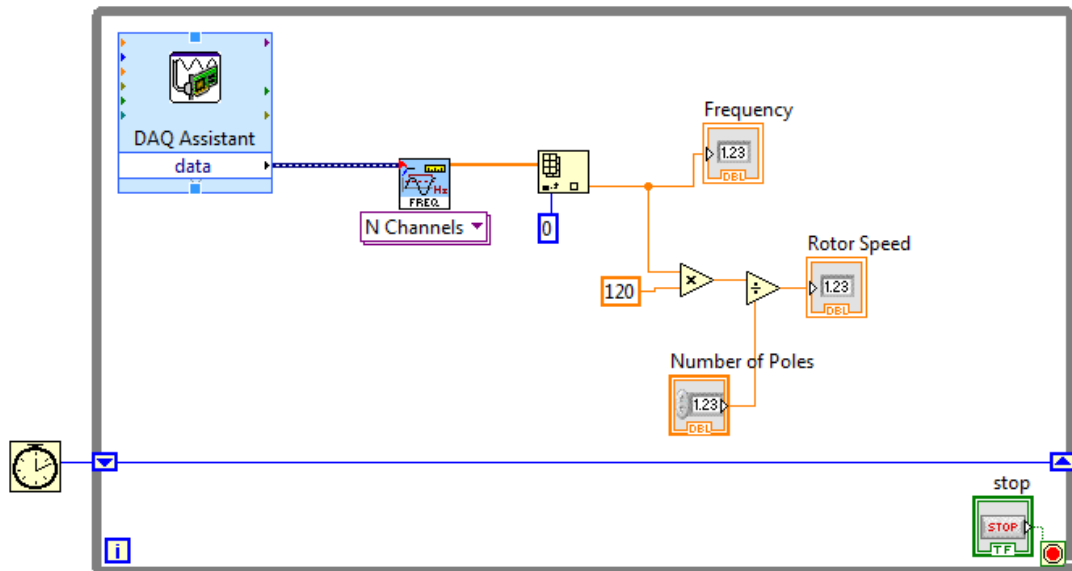


Figure 3.20: Block Diagram of DAQ for VAWT Rotor Speed



Figure 3.21: Measuring the rotor's speed of VAWT through Tachometer

Once the wiring connection and DAQ program were ready, the industrial fans were turned on to let the VAWT rotate. The speed of the rotor was measured by a tachometer as shown in Figure 3.21 after 10 minutes. The time was waited for 10 minutes to ensure the rotor speed of the VAWT is in a stable status. The reading adopted from the tachometer was compared with the reading shown in the LabVIEW user interface. The number of poles was adjusted to adopt the closest value of rotor speed with the one measured by the tachometer. The process was repeated with different speeds of industrial

fan to verify the speed adopts from DAQ is certain with the speed adopts from tachometer.

3.6.2 Test the performance of VAWT

The performance of VAWT was tested through the DAQ method which was similar as previous section. The equipment used for this section was included two industrial fans, a voltage card (model NI 9225), a current card (model NI 9227), an USB chassis (NI cDAQ-9174), current transducer platform and current transformer.

First of all, the height of both industrial fans was adjusted to be the same height with the centre of VAWT rotor. The distance between VAWT and fans were arranged to be closely as possible as shown in Figure 3.22. The wiring connection diagram for testing purpose is shown in Figure 3.24. In Figure 3.24, a full bridge rectifier was used to convert the AC form power into DC form. The output of rectifier was connected to the load that is represented by 50W variable pure resistor. While, the block diagram for DAQ is shown in Figure 3.25. The block diagram was designed to adopt and store data for each 30 seconds.



Figure 3.22: Testing of VAWT Performance



Figure 3.23: 50 watt (10 ohm) Variable Resistor

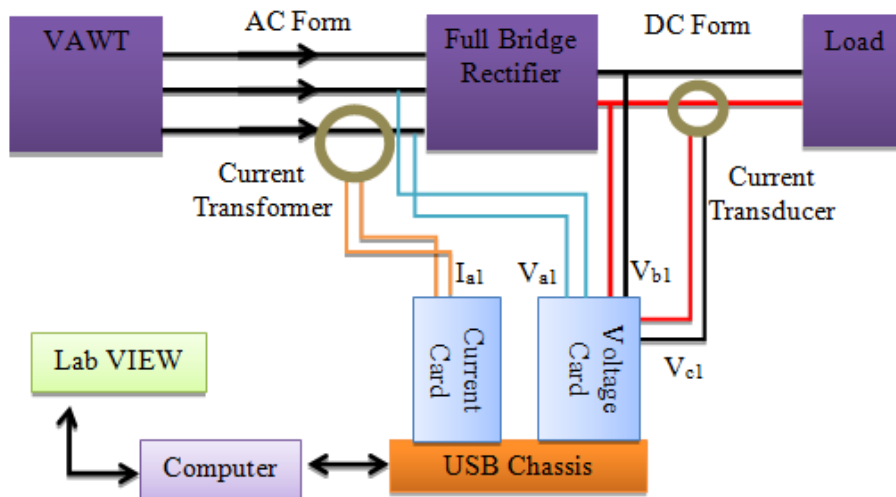


Figure 3.24: Wiring Connection Diagram for VAWT

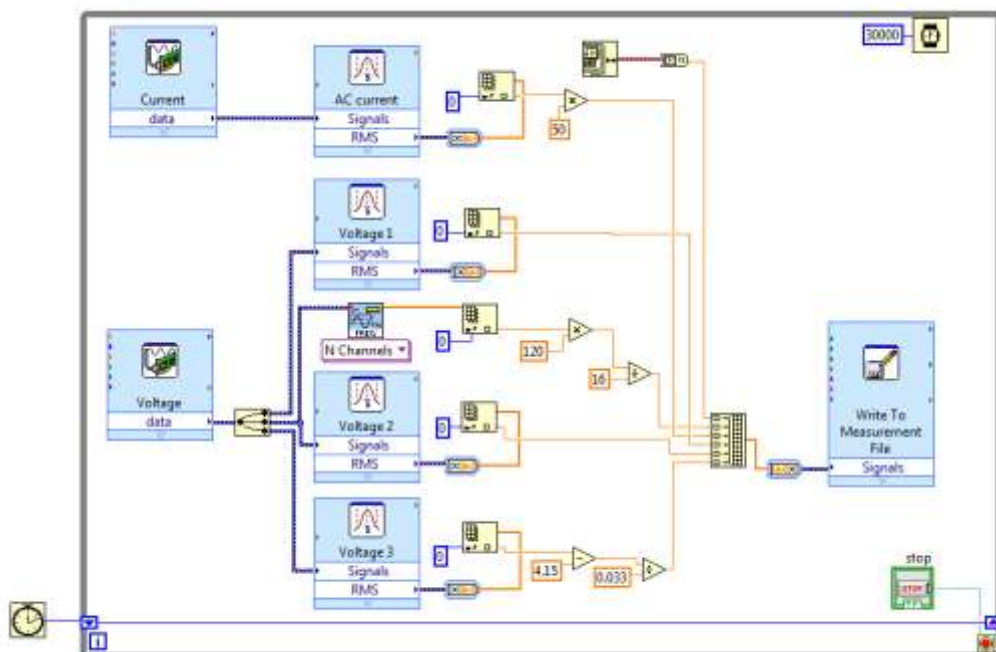


Figure 3.25: Block Diagram of DAQ for VAWT Performance Test

Several experiments were performed with the same DAQ platform and program as shown in previous paragraph. All the experiments had done at in door to avoid natural wind affects to the rotor speed. The results obtained from the experiences were processed in program Microsoft Excel and it is shown in Chapter 6. The detail procedures of these experiments are written as following subsection.

3.6.2.1 Experiment 1 – Fixed load with variable wind speed

The experiment 1 was conducted by fixing the resistance of resistor and tests the performance of VAWT with different level of wind speed. First, the resistor was adjusted to a fixed value and the resistance was measured through the multimeter. Then, the industrial fans were turned on with lowest speed and the collection of data was started. The steps were repeated after 10 minutes with different speed of industrial fans.

3.6.2.2 Experiment 2 – Variable load with fixed wind speed

The experiment 2 was conducted by fixing the speed of fan and tests the performance of VAWT with different level of load applied. First, the resistor was adjusted to a fixed value and the resistance was measured through the multimeter. Then, the industrial fans were turned on with maximum speed and the collection of data was started. The steps were repeated after 10 minutes with different level of resistance.

CHAPTER 4

PHOTOVOLTAIC SYSTEM

4.1 Overview of Photovoltaic (PV) System

This section will be briefly described the mechanism and the function of each main component in the photovoltaic (PV) system. In this project, the PV system was formed by a solid structure to locate an amount of PV modules, two string of PV array, 2 set of switchboard, 2 set of inverter and on-grid control panel. The overview of PV system in this project is shown in Figure 4.1. Basically, the PV systems are adopting the sun energy and convert it to the electrical energy. This electrical energy was connected to a grid system through the inverter before it was supplied to the consumer. The detail information about each component were studied and investigated as following sections.

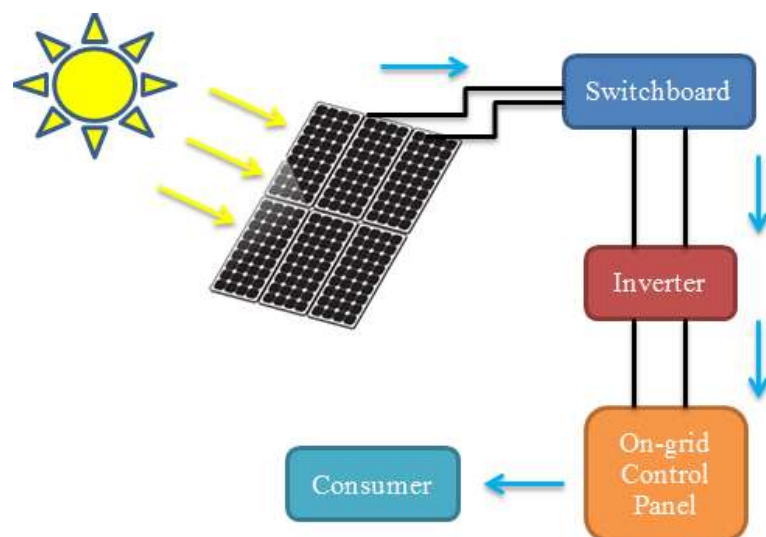


Figure 4.1: Overview of PV System

4.2 Installation PV system

The installation of PV system had done by the contractor. However, the installation processes were monitored for better understands of the PV system. The installation processes for PV system are shown in Figure 4.2 and Figure 4.3.



Figure 4.2: Installation of PV Structure



Figure 4.3: Installation of PV System

4.3 Construction of PV

The construction and design of PV were explained in this section. In this project, there was total of 32 set of PV modules. The front and back view of PV modules were shown in Figure 4.4. These PV modules were basically formed by internal connection of 60 set of Monocrystalline solar cells.



Figure 4.4: PV Modules

There were 4 set of PV array formed by these PV modules. Each set of PV array was formed by 8 set of PV modules through series circuit connection with each other to gain the output voltage. Then, two strings were formed by these PV array. Each string was formed by 2 set of PV array through parallel circuit connection with each other to gain the output current. The PV strings are shown in Figure 4.5.



Figure 4.5: PV Modules in UTAR

From the appendix K, each module had ability to create maximum power voltage (V_{mp}) of 29.4 Volts, maximum power current (I_{mp}) of 7.83Amps and maximum power (P_{max}) of 230 Watt. The open circuit voltage (V_{OC}) is 37 Volts and short circuit current (I_{SC}) is 8.42 Amps. All these values were based on 1000W/m^2 irradiance with cell temperature of 25 degree Celsius as stated in appendix K. By having these values, the calculation can be made to estimate the maximum production of power, voltage and current for each string. The maximum power produces by each string is expressed as

$$\begin{aligned} P_{max1} &= \text{no. of PV modules in the string} \times P_{max} \\ &= 16 \times 230 \\ &= 3680 \text{ W} \end{aligned} \quad (4.1)$$

where

P_{max1} = PV string maximum power, W

P_{max} = PV module maximum power, W

The maximum voltage produces by each string is expressed as

$$\begin{aligned} V_{max1} &= \text{no. of PV modules in single array} \times V_{OC} \\ &= 8 \times 37 \\ &= 296 \text{ V} \end{aligned} \quad (4.2)$$

where

V_{max1} = PV string maximum voltage, V

V_{OC} = PV module open circuit voltage, V

The minimum voltage produces by each string is expressed as

$$\begin{aligned}
 V_{min1} &= \text{no. of PV modules in single array} \times V_{mp} \\
 &= 8 \times 29.4 \\
 &= 235.2 \text{ V}
 \end{aligned}
 \tag{4.3}$$

where

V_{min1} = PV string minimum voltage, V

V_{mp} = PV module maximum power voltage, V

The maximum current produces by each string is expressed as

$$\begin{aligned}
 I_{max1} &= \text{no. of array in the string} \times I_{sc} \\
 &= 2 \times 8.42 \\
 &= 16.84 \text{ A}
 \end{aligned}
 \tag{4.4}$$

where

I_{max1} = PV string maximum current, A

I_{sc} = PV module short circuit current, A

The energy produces by each string is expressed as

$$\begin{aligned}
 E &= \text{no of hour PV panel receive direct sun shine} \times P_{max1} \\
 &= 4 \times 3680 \\
 &= 14.72 \text{ kWh}
 \end{aligned}
 \tag{4.5}$$

where

E = energy of PV system produced in a day, kWh

P_{max1} = PV string maximum power, W

Based on these results, the maximum power produced by each string was up to 3.68 kW with the operating voltage range of 235.2 - 296 Volts DC. The maximum current of each string was up to 16.84 Amps DC. The energy produces in a day was 14.72 kWh with operation hour of 4.

4.4 Switchboard and Inverter

The Figure 4.6 had shown the external and internal view of PV switchboard. This switchboard was contained the switches and the fuses. The switches were used to connect/disconnect the PV output array to the inverter. Besides, it also acts to connect/disconnect the two set of array to form a string. The fuses were used as protection in case of system failure. The output of switchboard was connected to the inverter through the wires.

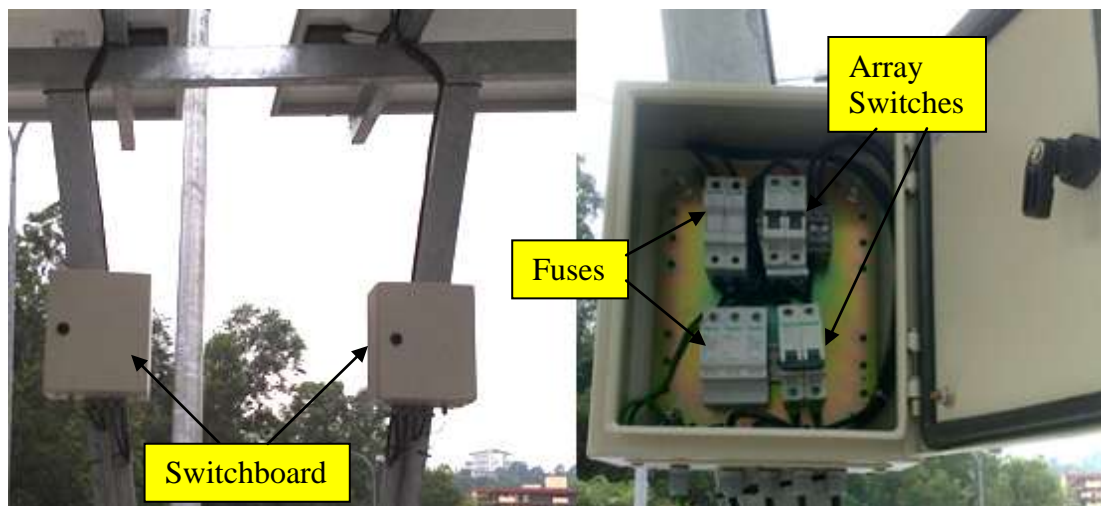


Figure 4.6: PV Switchboard

Basically, the inverter acts as a converter to convert the DC power into AC power. However, the inverter used in this project had the ability to track the maximum power point of the PV array to improve the power before feeding the output power into the grid system. There were two sets of string inverters (model TL 3) used in this project and the detail specification is shown in appendix C and D.

Based on the Figure 4.7, the LCD display was used to display the reading of power and terminal (negative and positive) was connected with the PV output.

From the Appendix C and D, the inverter had input voltage range of 120 – 500 V DC and MPPT operating input voltage range of 150 – 500 V DC. These values mean any incoming voltage less than 120 V DC, the inverter is not producing any output power. The maximum input current can supports is up to 22 A DC and the maximum output current is up to 13 A AC. The maximum output power is up to 3 kW.



Figure 4.7: PV Inverter

The output terminal of inverter was connected to the main control panel as shown in Figure 4.8. The connection of grid system and the control panel had done by the grid cable as shown in Figure 4.8 and 4.9. The switches on the control panel and main switchboard will be used to on/off the inverter feed to the grid system.

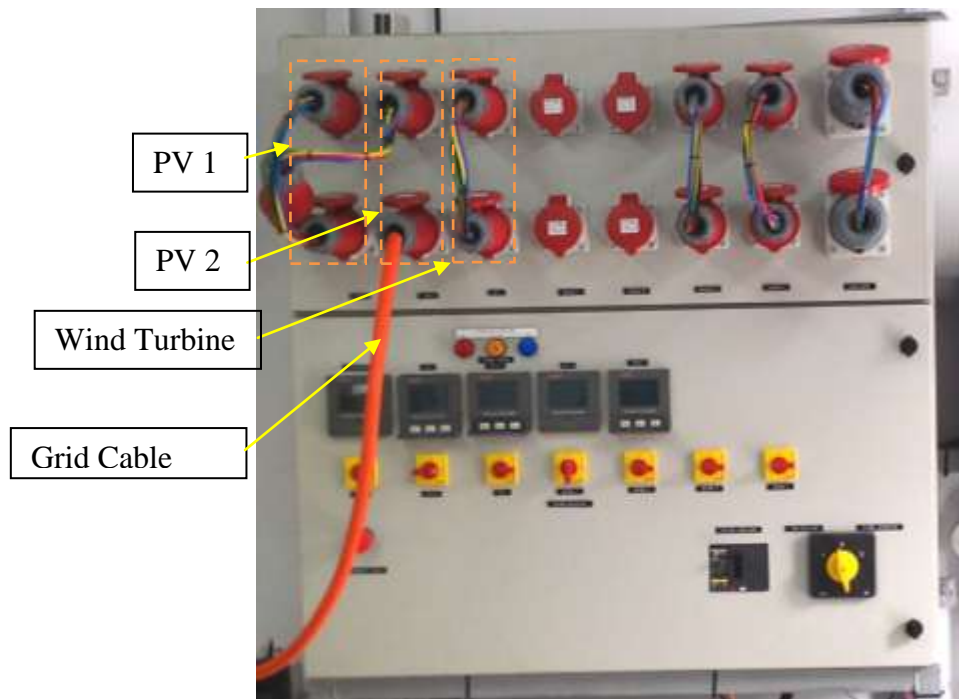


Figure 4.8: Control Panel

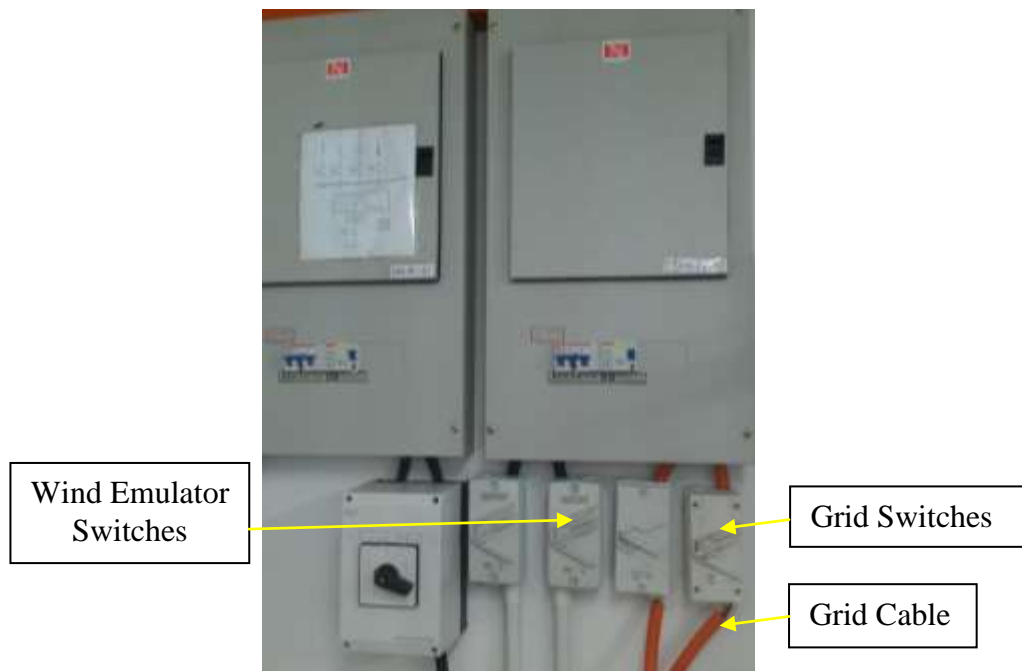


Figure 4.9: Main switchboard

CHAPTER 5

WIND TURBINE SYSTEM

5.1 Wind Turbine

This section will briefly describe the connection, mechanism and operating system of wind turbine system. In this project, there were two type of wind turbine involved. There were Horizontal Axis Wind Turbine (HAWT) and Vertical Axis Wind Turbine system (VAWT). The operating systems of both wind turbines were different. The output of HAWT was feeds to the grid system while VAWT was operated in off grid mode.

Other than that, the wind emulator was also involved in this project. The wind emulator was used to simulate the operation of wind turbine in case the wind stream is not strong enough to support the wind turbine. The details of each wind turbine and wind emulator are written in following section.

5.1.1 Horizontal Axis Wind Turbine (HAWT) System

Generally, the HAWT is a machine that generates electricity by adopting the energy the natural wind. However, a system was built to allow the HAWT to produce maximum electrical power to feed to the grid system. The overview of HAWT system is shown in Figure 5.1.

The HAWT system used in this project can be separate into two parts which were mechanical and electrical. The mechanical parts shown in Figure 5.2 were including tower, nacelle, yaw, brake system, blades and shaft. On the other hand, the electrical parts were including generator, flight controller and inverter.

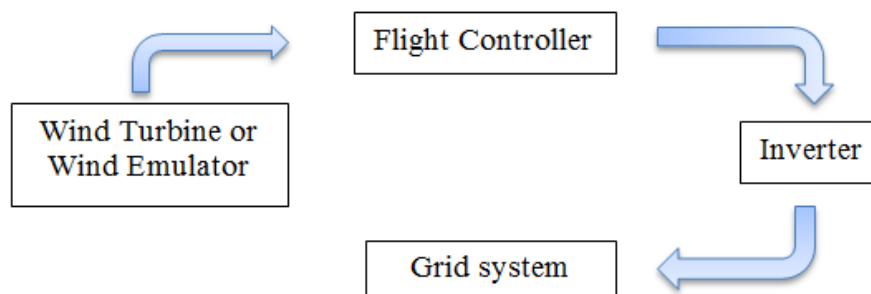


Figure 5.1: Overview of HAWT system

5.1.1.1 Horizontal Axis Wind Turbine (HAWT)

The Figure 5.2 has shown the HAWT in this project. The wind energy was adopted through the blades and the blades were rotating together with the rotor. Inside the nacelle, the rotor was connecting with the shaft of generator. As the blades were rotating, the linear kinetic energy adopts from wind was converting to the mechanical energy. This mechanical energy was transferred into electrical energy through the generator inside the nacelle.

The design of X wind chassis allows the wind turbine to capture the direction of wind blow and change the direction through the yaw. This was important as the maximum wind energy was adopted when the blades are 90 degree perpendicular angle with the wind stream. From the Appendix L, the HAWT used in this project was downwind type. The downwind type allows the wind energy to be adopts from the backside of wind turbine. Hence, the wind stream will first flow through the X wind chassis to change the direction of wind turbine before rotates the blades.

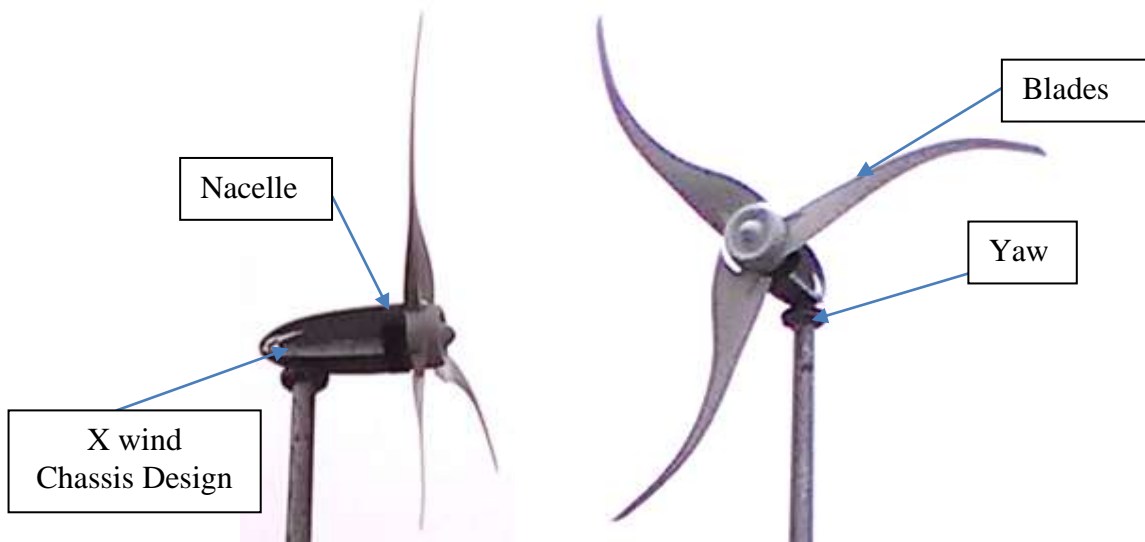


Figure 5.2: HAWT (left side is side view and right side is front view)

From the Appendix L, the 3 phase permanent magnet generator was used in this HAWT and the output was 3 phase AC power. The connection of generator was in star connection circuit as four wires were present. The minimum wind speed (cut in speed) requires to generate an output power was 3 m/s while the rated output power was 1100 kW at the speed of 8 m/s. The rotor and generator were rotating in variable speed mode as natural wind stream was changing all the time. Hence, the output voltage and current were varying in magnitude and frequency. These variable output was unable to direct feed to the grid system. Therefore, other devices such as flight controller and inverter were needed as written in next section.

5.1.1.2 Wind Emulator

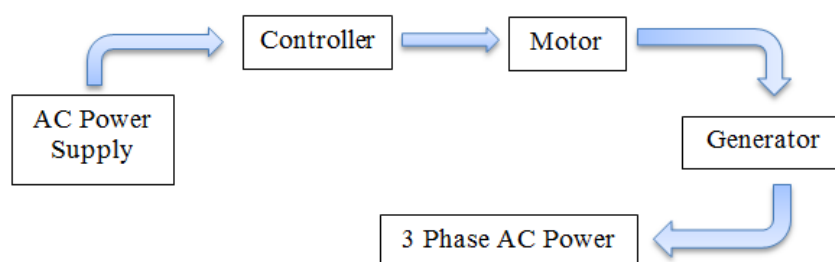


Figure 5.3: Overview of Wind Emulator System

The Wind Emulator is simulator of wind turbine. It was used to duplicate the function of wind turbine to generate electrical power. It was operated when the condition of wind stream was not ideal. The overview of wind emulator is shown in Figure 5.3. The wind emulator was formed by a speed controller, motor and generator. The generator was directly attached with the motor as shown in Figure 5.4. In Figure 5.5, the controller is used to control the speed of motor and indirectly control the output power of generator. The output of generator was 3 phase AC power with star connection circuit as four wires are present.



Figure 5.4: Generator and Motor of Wind Emulator



Figure 5.5: Wind Emulator's Controller

5.1.1.3 Flight Controller

Basically, the flight controller used in this project is acts as controller, converter and protector of the HAWT system. The picture of flight controller and inverter are shown in Figure 5.6. This flight controller was allowing the operator to control the operation of HAWT either off or on. The conversion of 3 phase AC power into DC power was done by converter and the HAWT system was protected by the protector from the system overload or over speed. The detail mechanism of flight controller were studied, investigated and written in next few paragraphs.



Figure 5.6: Flight Controller and Inverter

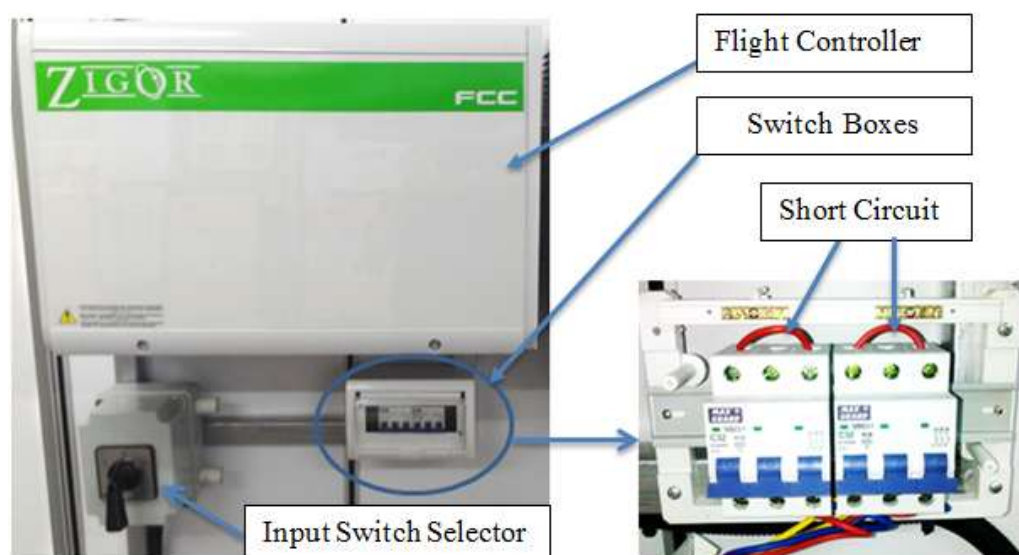


Figure 5.7: Overview of HAWT control system

The overview of HAWT control system is shown in Figure 5.7. In the Figure 5.7, the output of generator and wind emulator were both connected to an input switch selector. The output of this input switch selector was connected to the flight controller. This input switch selector was built to allow the operator to select the input for flight controller. There were three selections which were off mode, wind turbine and wind emulator.

In Figure 5.7, the switchboards were connected parallel with the output of generator and wind emulator inside the input switch selector. Inside the switchboards, either two phase of the input phase were short circuit to stop the wind turbine from rotating.

The interior view of flight controller is shown in Figure 5.8 and each main components was labelled with numbers for further explanation as following:

- 1- Main input AC power (240 V 50 Hz) source is used to supply components 4 and 6.
- 2- Isolation transformer with ratio 1:1 is used to reduce the noise in power lines before the main AC power passed through other components.
- 3- A fuse is used to protect the whole system.
- 4- An adaptor or converter is used to supply 24 V DC power for components 5 and 10 .
- 5- A xLogic SuperRelay is used to control the switching of components 6b and 6c. The xLogic SuperRelay is a compact and expandable CPU replacing mini PLCs, multiple timers,relays and counters. This xLogic SuperRelay is programmed to trigger the component 6c (stop the wind turbine) and trigger the component 6b (allow some current flow through the dump load) when the output current is over the pre-set limit. Hence, its works as controller and protection in this system.
- 6- Three set of power relays are used to work as switches to either connect or disconnect the input power with other components . All the input source for these power relays are connecting with component 11. The output terminal of

- Component 6a is connecting with component 8 and its controlled by power source.
 - Component 6b is connecting with component 9 and its controlled by component 5.
 - Component 6c is short-circuit to shut down the wind turbine and its controlled by component 5.
- 7- Input power (3 phase) from input switch selector
- 8- A three phase rectifier is used to convert AC power into DC power. This rectifier provides the output DC power for inverter in figure 5.7.
- 9- A three phase rectifier is used to convert AC power into DC power. This rectifier provides the output DC power for dump load in figure 5.9.
- 10- A DC Hall Effect Current Transducer is used to measure the output DC current and output an dc voltage signal which is proportional to input current signal. The output voltage is connected to component 5 as input reference.
- 11- A switches is used either connect or disconnect the flight controller from the input power 7.

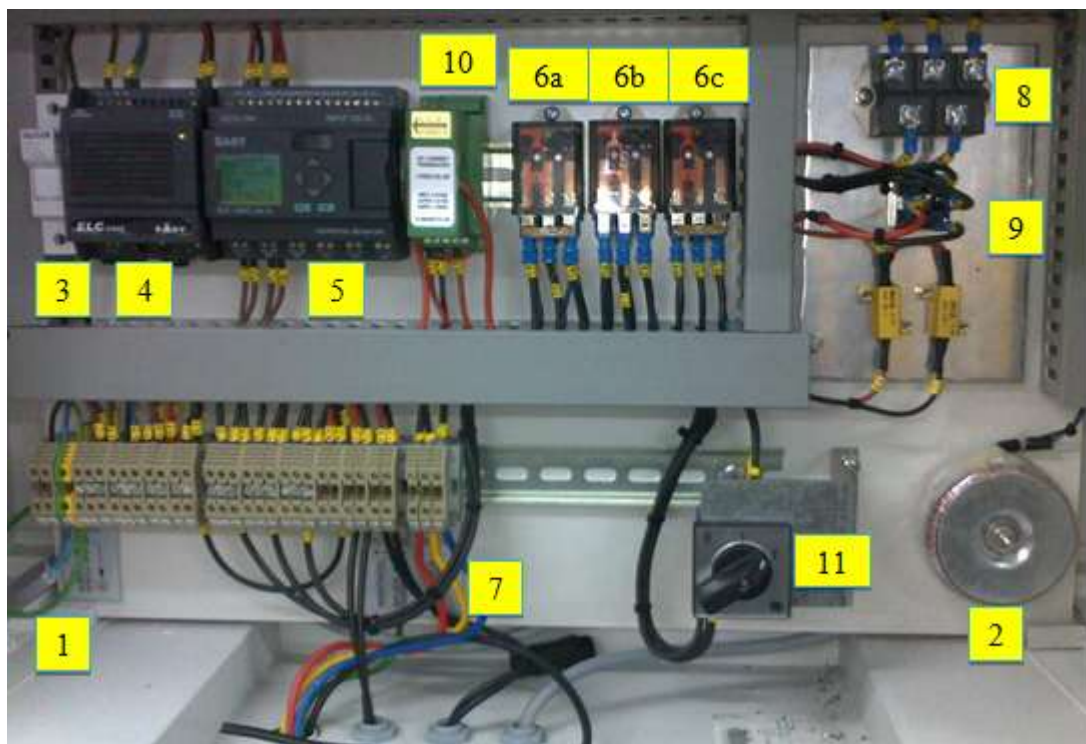


Figure 5.8: Interior View of Flight Controller



Figure 5.9: Dump Load

The inverter model WINDZET SP2 K shown in Figure 5.7 is used in HAWT system. The inverter was used to convert DC power in AC power. Besides, its also regulates the frequency and voltage in order to feed to the grid system. Other than that, it also had ability to track maximum power point (MPPT) to improve the output power. With the feature of MPPT, the speed of HAWT was indirectly controlled by the inverter. This MPPT was able to adjust the amount of current draws from HAWT and indirectly affect the amount of torque applied on the generator.

Based on the manufacture datasheet, the inverter was able to produce nominal output power of 2 kW. The inverter able to support maximum input voltage up to 500 V DC and maximum input current of 18A DC. The MPPT voltage range were 150 – 370 V DC. Therefore, the speed of HAWT was under control of inverter when the incoming voltage was within the range of MPPT.

The input terminal (DC power) was connected to the Flight Controller. While, the output terminal (AC power) was connected to the control panel as shown in figure 4.8. The connection of grid system and the control panel had done through the grid cable as shown in Figure 4.8 and 4.9.

5.1.2 Vertical Axis Wind Turbine (VAWT)

The connection and operating system of VAWT were mostly similar with HAWT system. The main different for HAWT and VAWT were their axis (main shaft) about which the rotating parts was revolved. In this project, the VAWT was used for off-grid purpose which means the output power was directly connected to the load instead feed to the grid system. Therefore, it's much simple compared to the HAWT. The overview of VAWT system is shown in Figure 5.10. The VAWT system was formed by VAWT, charge controller, battery and load.

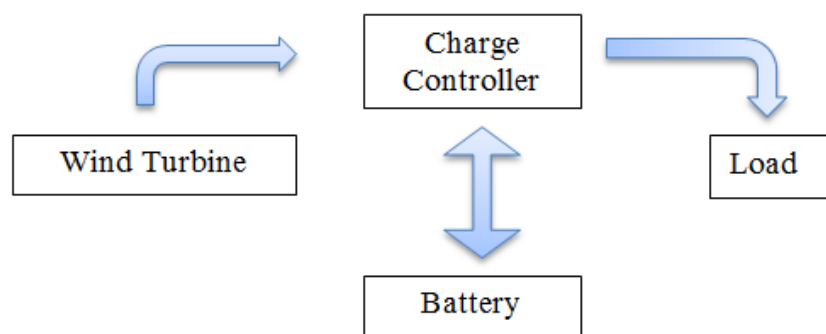


Figure 5.10: Overview of VAWT System

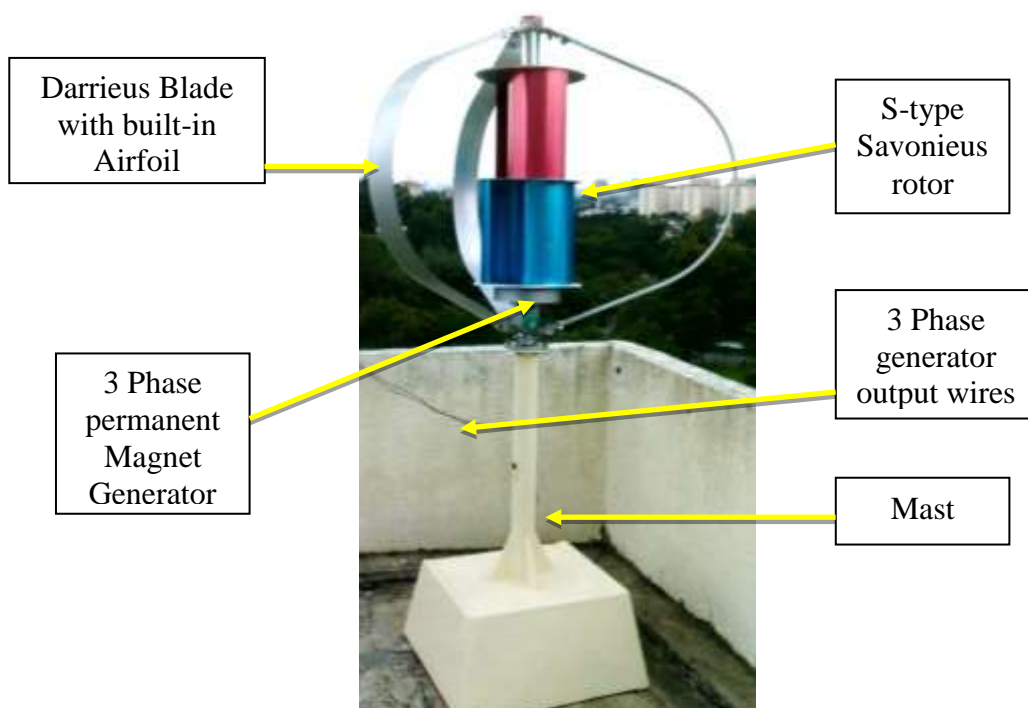


Figure 5.11: Vertical Axis Wind Turbine (VAWT)

The VAWT used in this project is shown in Figure 5.11. In the Figure 5.11, each main component was labelled as expressed as following:

- 1- A S-type Savonius rotor acts to adopt wind energy and rotate the rotor.
- 2- 3 set of Darrieus Blade with built-in Airfoil are designed to improve the speed of rotor.
- 3- A 3 Phase permanent Magnet Generator is attached with rotor to rotate together and generate 3 phase AC electrical power. The connection of generator is in delta connection circuit as only three wires are present. Based on the manufacture label, the generator is output power is rated at 400 Watts.
- 4- A 3 Phase generator output wires are connects to the charge controller as shown in figure 5.13.
- 5- A mast is used to holds or locates the HAWT in place.

The charge controller and wiring connection of charge controller are shown in Figure 5.12 and Figure 5.13. The charge controller acts like center unit to connect VAWT, battery and load with each other. The type of charger controller used in this project were wind and solar hybrid controller. This controller had two input source (wind turbine and solar panel), battery input and two output load.



Figure 5.12: Charge Controller and Battery

This charge controller works as a converter, a voltage regulator and a charge controller. It helps to convert the AC 3 phase power from VAWT into DC power. The DC voltage was regulated before charging the battery or supplied to the load. Hence, the output power was always a fixed DC voltage. This controller has the capability to charge the battery without spoiling the battery by sensing the battery's voltage level.

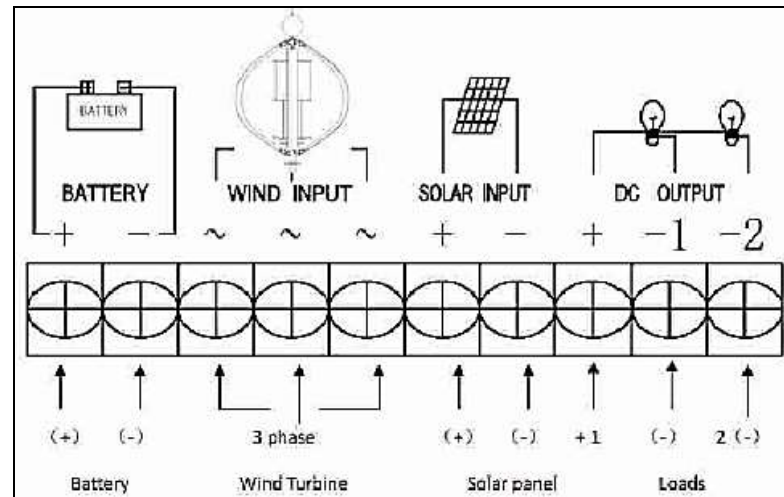


Figure 5.13: Wiring Diagram of the Controller's Terminal (TIMAR Technology Co.,Ltd)

On the other hand, the charge controller was intelligence enough to automatic stop the VAWT by short circuit internally if the input source voltage was over limit. It also intelligence to automatic trigger the power supply to the load based on the battery's voltage level and timing that pre-set by operator.

The LCD of the controller was used to indicates the information of input source (voltage, current, power and speed of rotor), battery voltage, output load (voltage, current and power) and some setting to trigger the output load either by voltage level or timer.

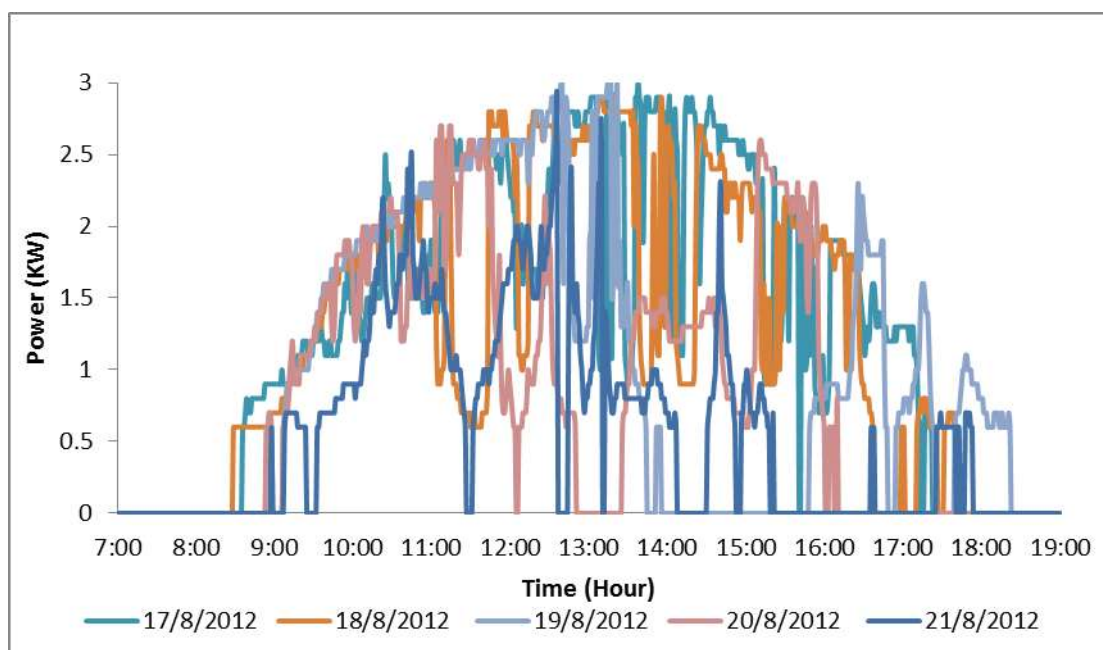
CHAPTER 6

RESULTS AND DISCUSSIONS

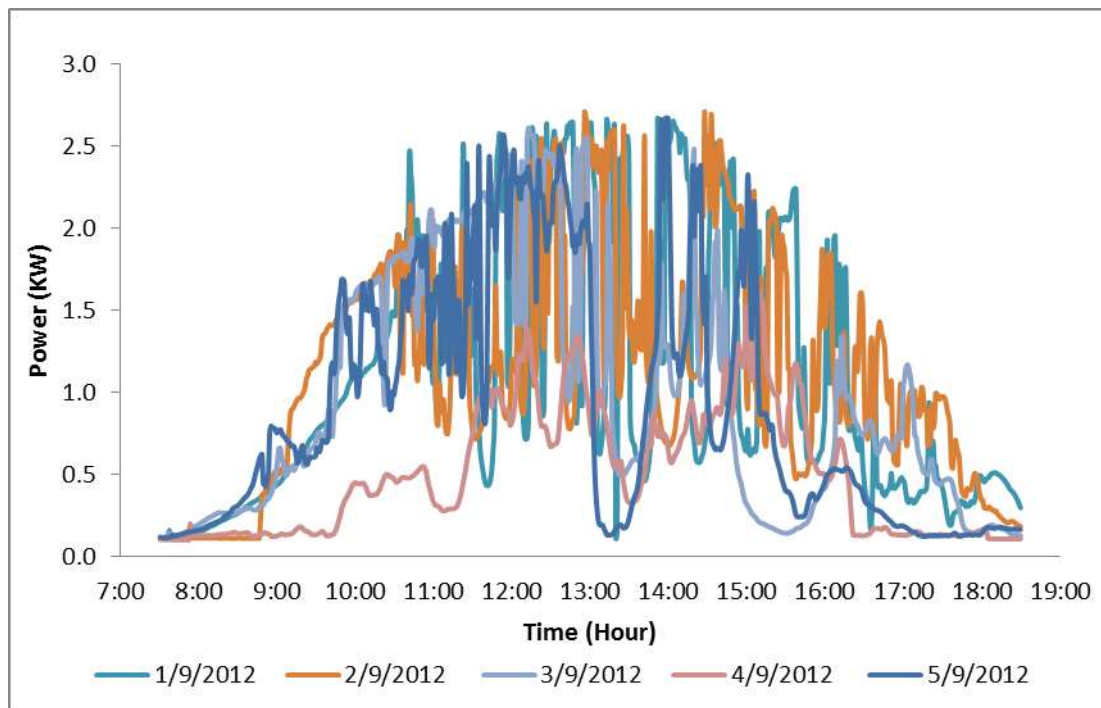
6.1 Comparison of Power Analyzer and DAQ platform

In the Chapter 3, two approaches were used to determine the inverter output power. Both approaches were successful to collect the data from the inverter. The accuracy of these approaches were compared based on the results adopt from each approach. These results were presented in the Graph 1 and Graph 2.

Graph 1: PV Inverter Output Power (kW) versus Time (Hour) through Power Analyzer



Graph 2: PV Inverter Output Power (kW) versus Time (Hour) through DAQ platform



The Graph 1 has shown the results adopted by Power Analyzer and Graph 2 has shown the results adopted by DAQ platform. Both graphs were plotted as the PV Inverter Output Power versus Time. The graphs were plotted from 7:00 am to 7:00 pm as the power generated after or before these periods were smaller than 0.1kW.

Based on these graphs, the starts and end time of power generated by PV system was different. In Graph 1, the power started to generate at 8:30 am and the amount of power generated started from 0.6kW. In Graph 2, the start time of power been generated was around 7:30 am and the amount of power generated started from 0.1 kW.

Hence, the results obtained from the DAQ platform was much reliable than power analyzer as it was not generally for PV system to generate power directly from 0.6kW instead of few Watt power. The reason for power analyzer to adopt power at minimum of 0.6kW may due to the limitation of current probe where it was only capable to sense at minimum current of 2.5 A AC.

Although, the accuracy of power analyzer was lower than DAQ platform but it still had advantages of simple wiring connection, lower cost and ease to set up. However, the approach of DAQ platform for data collection was still preferred in this project as it had higher accuracy. In addition, the DAQ platform had advantage to combine or display the output of 3 set inverters come from PV system and HAWT in a single program. This can be seen by using the program LabVIEW to design DAQ platform user interface. The program had made the life of operator ease as the monitoring system for both PV and HAWT system can be done in a single computer.

6.2 PV Output Profile

The accuracy of DAQ platform was better than power analyzer. Therefore, the PV output profile was done by the approach of DAQ platform. The PV output power was collected for 30 days (8/29/2012 – 9/27/2012). These data were processed in program Microsoft Excel to get the monthly output power profile.

Based on the Graph 2, the output power had a fixed pattern although the amount of power produced was varying with time. The pattern of power was obtained from the Graph 2. It shown the power started to increase from 7:30 am until 2:00 pm. After 2:00 pm, the power started to decrease until few watts at around 6:30 pm. These patterns were almost same for each day.

From the Graph 2, it also noticed that the PV system was still generating the power with very few watts at the night time. However, this can be understood as the PV system was generating the power from the light source of street light. In order to ignore the factor caused by the street light, the real production hour of PV system from the sun light was set to start from 7:30 am to 6:30 pm with total production hour of 11 hours.

The monthly output power profile of PV system was captured from Microsoft Excel as shown in Figure 6.1. Meantime, the daily output power profile of PV system was captured from Microsoft Excel as shown in Figure 6.2.

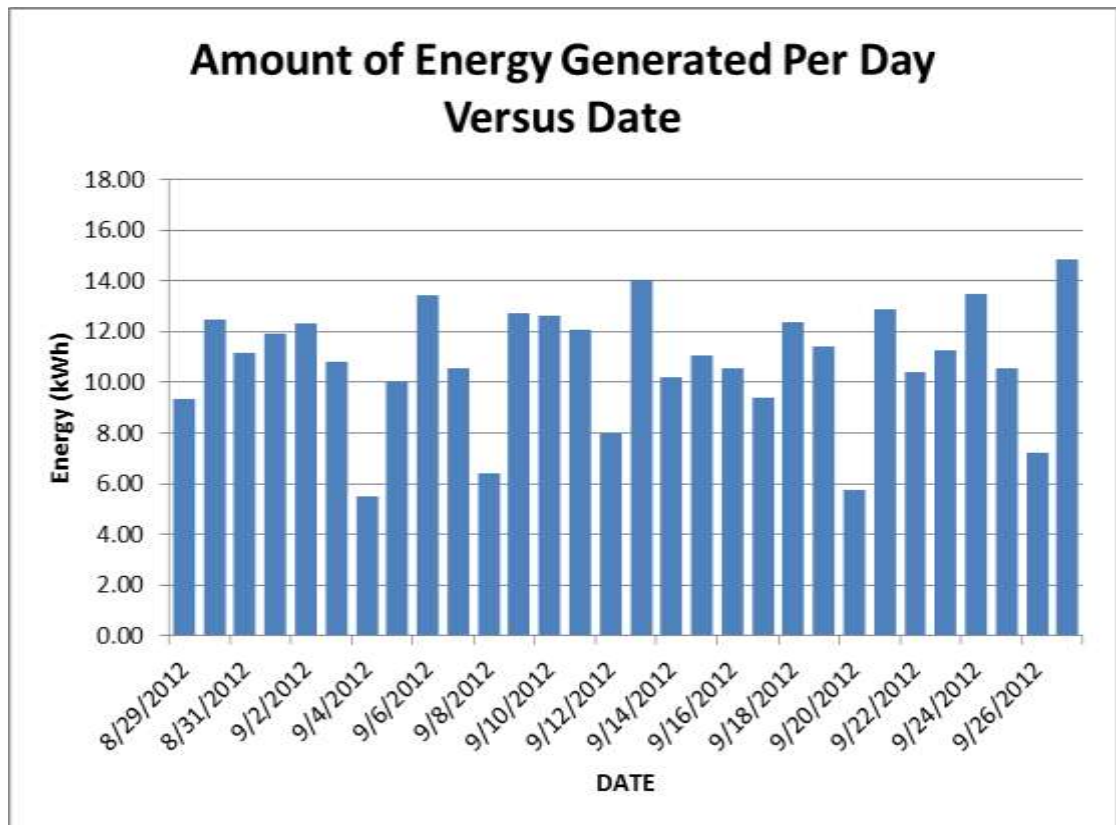
MONTHLY OUTPUT POWER PROFILE OF THE PV1			
Period	8/29/2012 - 9/27/2012		No. of Days
Peak Energy of the month	14.84 kWh	on	9/27/2012
Valley Energy of the month	5.52 kWh	on	9/4/2012
Total Energy of the month	324.63 kWh		
MAX Power of the month	2.830 kW	on	9/27/12 7:44 AM
MIN Power of the month	0.003 kW	on	9/24/12 7:43 AM
Less than 6 kWh per day	5 days		
Inbetween (8-11kWh) per day	9 days		
More than 11 kWh per day	16 days		

Figure 6.1: Monthly Output Power Profile of PV System

No.s	DATE	Average Power (kW-h)	Energy per day (kWh)	Based on Data 2 (PEAK MINUTE)				Based on Data 4 (PEAK HOUR)				Amount of Energy Generated per day (%) (MAX = 15 kW-h)
				MAX (kW-min)	Time (MAX)	MIN (kW-min)	Time (MIN)	MAX (kW-hour)	Time (MAX)	MIN (kW-hour)	Time (MIN)	
1	8/29/2012	0.85	9.35	2.62	11:41	0.00	14:07	1.75	12:00	0.21	8:00	62.32%
2	8/30/2012	1.13	12.47	2.76	12:58	0.13	17:54	2.10	13:00	0.15	18:00	83.11%
3	8/31/2012	1.01	11.16	2.57	11:03	0.11	8:16	1.87	11:00	0.13	8:00	74.39%
4	9/1/2012	1.09	11.94	2.66	13:51	0.11	7:36	2.05	13:00	0.17	8:00	79.57%
5	9/2/2012	1.12	12.30	2.71	14:27	0.11	8:46	1.89	13:00	0.11	8:00	81.99%
6	9/3/2012	0.98	10.78	2.61	12:12	0.11	7:34	2.19	12:00	0.20	8:00	71.88%
7	9/4/2012	0.50	5.52	1.62	15:09	0.10	7:51	1.08	15:00	0.12	8:00	36.80%
8	9/5/2012	0.91	10.04	2.67	13:59	0.12	7:36	2.05	12:00	0.15	18:00	66.91%
9	9/6/2012	1.22	13.42	2.70	13:26	0.12	7:30	2.09	11:00	0.18	8:00	89.44%
10	9/7/2012	0.96	10.53	2.70	12:07	0.11	7:49	1.63	13:00	0.15	8:00	70.18%
11	9/8/2012	0.58	6.41	2.72	13:39	0.10	7:32	2.05	13:00	0.12	8:00	42.76%
12	9/9/2012	1.16	12.73	2.74	12:21	0.11	8:37	2.22	13:00	0.11	8:00	84.88%
13	9/10/2012	1.15	12.60	2.68	12:11	0.12	7:30	2.40	13:00	0.21	9:00	84.00%
14	9/11/2012	1.10	12.08	2.70	14:35	0.10	7:30	2.21	15:00	0.19	8:00	80.54%
15	9/12/2012	0.73	7.99	2.67	12:46	0.10	7:30	1.78	13:00	0.14	8:00	53.29%
16	9/13/2012	1.28	14.05	2.63	11:37	0.09	7:30	2.01	11:00	0.22	8:00	93.64%
17	9/14/2012	0.93	10.18	2.51	15:33	0.10	7:32	1.69	14:00	0.21	8:00	67.86%
18	9/15/2012	1.00	11.04	2.64	11:10	0.11	7:32	1.94	11:00	0.15	13:00	73.57%
19	9/16/2012	0.96	10.54	2.74	13:59	0.10	7:57	1.65	14:00	0.11	8:00	70.28%
20	9/17/2012	0.85	9.37	2.36	12:31	0.10	18:24	1.90	13:00	0.12	8:00	62.46%
21	9/18/2012	1.13	12.39	2.57	12:53	0.10	7:32	2.28	13:00	0.22	8:00	82.59%
22	9/19/2012	1.04	11.43	2.53	12:57	0.11	7:33	2.09	13:00	0.20	8:00	76.17%
23	9/20/2012	0.52	5.74	2.35	13:34	0.10	7:40	0.95	11:00	0.13	17:00	38.30%
24	9/21/2012	1.17	12.87	2.77	12:56	0.10	18:07	1.89	11:00	0.19	18:00	85.77%
25	9/22/2012	0.95	10.41	2.73	13:31	0.10	17:48	1.86	13:00	0.14	18:00	69.42%
26	9/23/2012	1.02	11.24	2.73	12:32	0.10	7:48	1.93	11:00	0.15	8:00	74.93%
27	9/24/2012	1.22	13.46	2.82	13:37	0.09	7:32	2.26	12:00	0.17	8:00	89.73%

Figure 6.2: Daily Output Power Profile of PV System

Based on Figure 6.1 and Figure 6.2, the total energy produced by a PV system was 324.63 kWh in 30 days and it was based on 11 hours of production per day. The range of energy generated in a single day was 5.52 – 14.84 kWh. There were 25 days out of the 30 days the energy generated in a single day was more than 8 kWh per day. Hence, the 11kWh can be considered as average energy produce in a day.

Graph 3: Amount of Energy Generated per Day versus Date

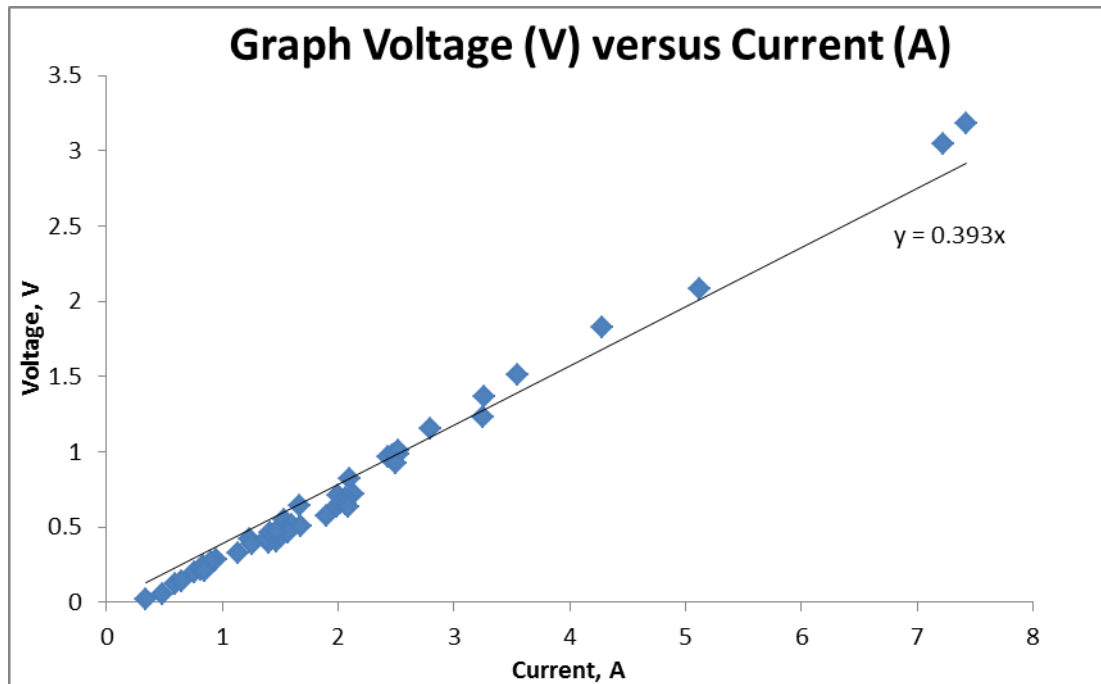
Based on the Graph 3, it was obtained that the amount of energy produced by PV system in each day was different. This can be explained as PV output power varies with the solar irradiance and the solar irradiance varies all the time. It also depends on the weather. The maximum energy was produced in sunny days while the minimum energy was produced on rainy days. Hence, it was not possible to get a constant energy throughout the day.

6.3 Power losses along the Wires in PV system

The results adopted in Section 3.4.2 were processed in the program Microsoft Excel and the graph 4 was plotted. The graph had shown the relationship between voltage and current as a linear graph. The current was increased as the voltage was increased. The relationship between voltage (V) and current (I) was expressed in equation as shown

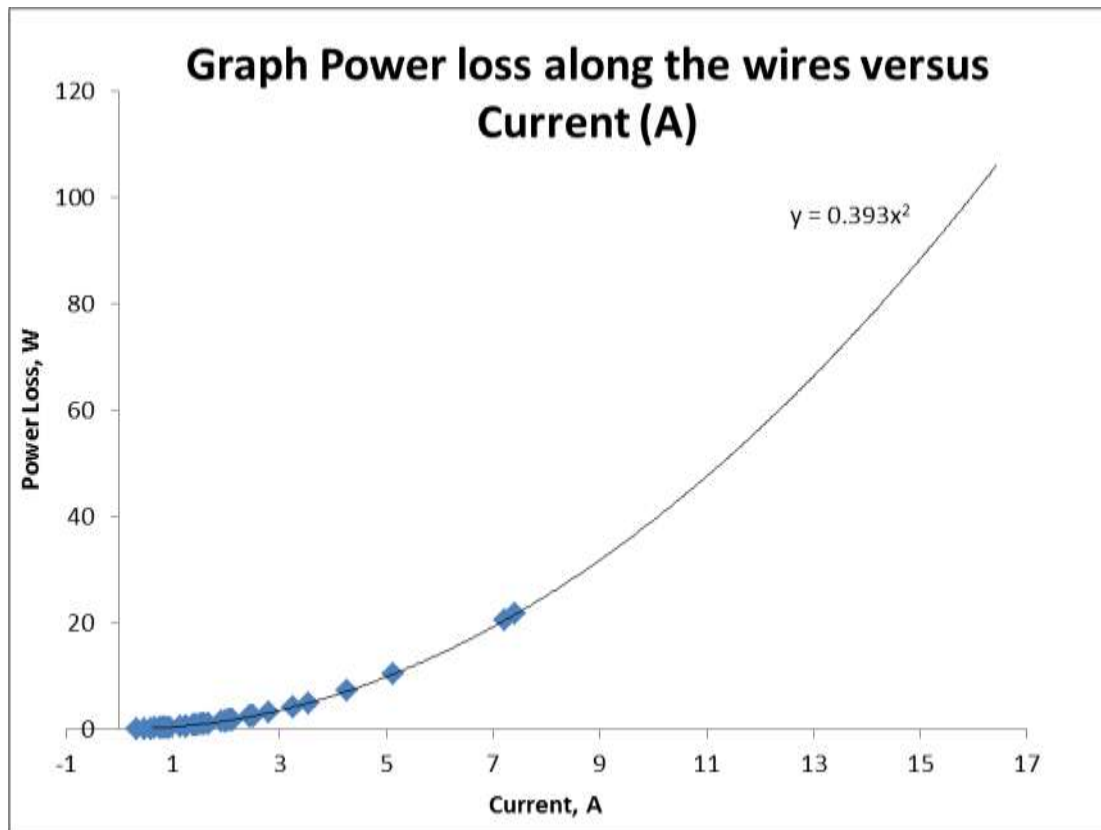
in the graph. By compares this equation with the ohm's law equation. It was found that the value 0.393 was referred to resistance along the wires.

Graph 4: Voltage drop along the Wires (V) Versus Current (A)



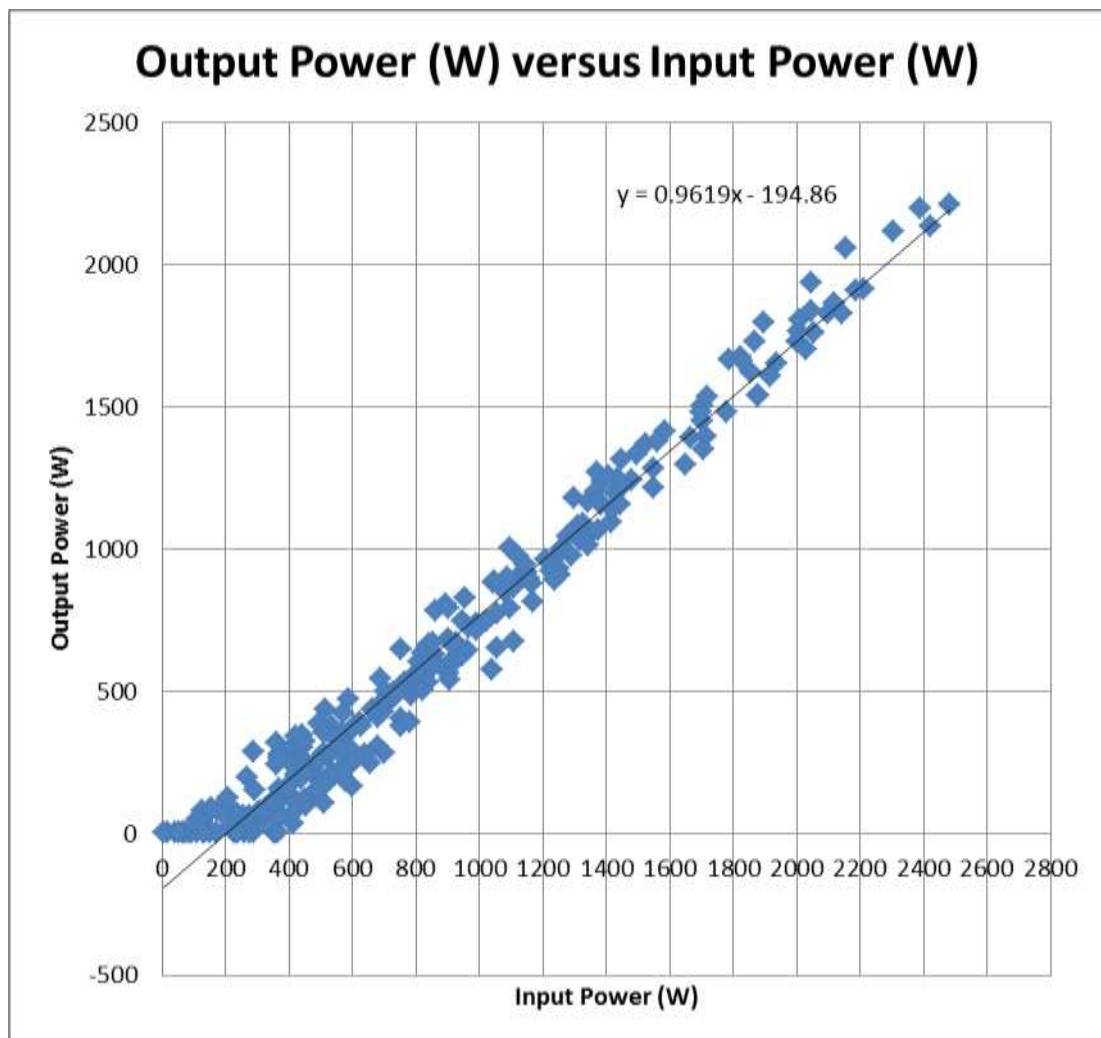
Hence, the power losses along the wires can be calculated based on the joule's law equation. The Graph 5 was plotted based on the equation of joule's law. It was obtained that the power loss along the wires was increased as the current was increased. In the Chapter 4, the maximum current produced by the single string of PV array was 16.84 A. Therefore, the maximum power loss along the wires could be up to 111.45 Watts at the maximum current state. From the Section 6.2, the maximum power generated by the single strings of PV array was 2.83 kW. Then, the calculated percentage of power loss along the wires was about 4% with the equation 3.2.

Graph 5: Power loss along the Wires (W) Versus Current (A)



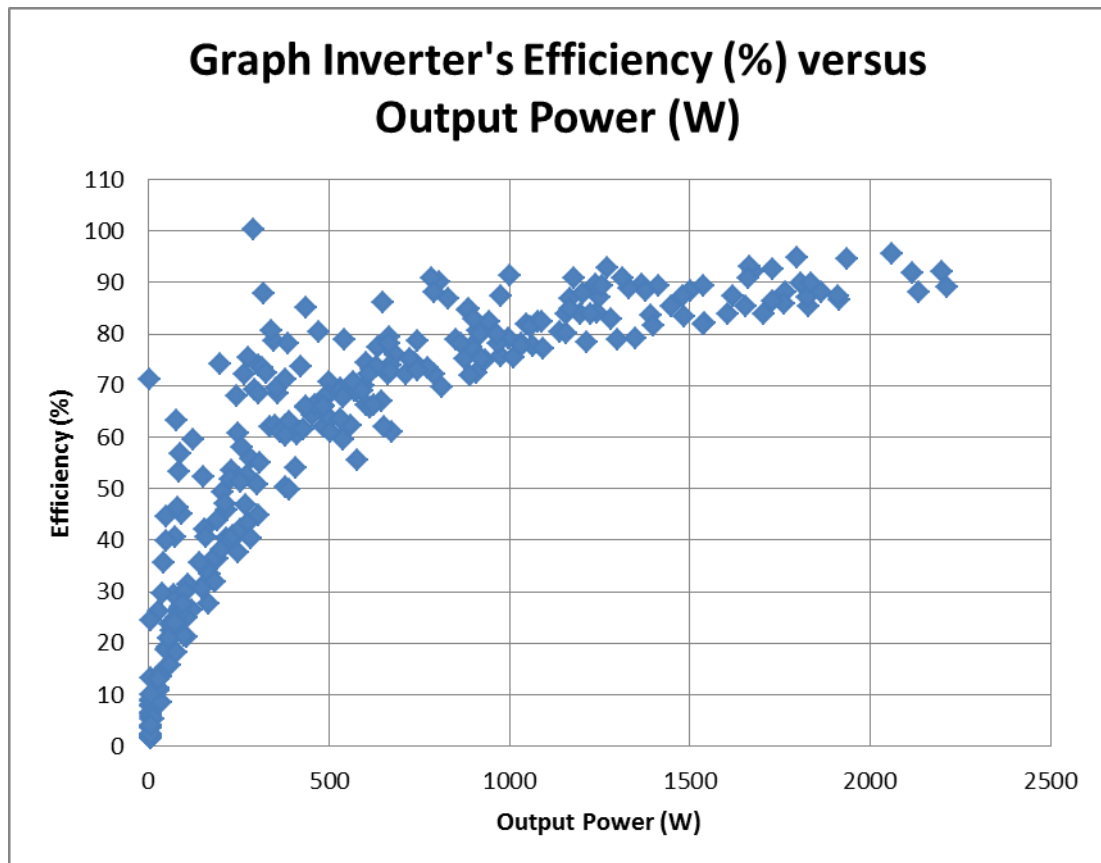
6.4 Power losses in the PV Inverter

The results of inverter either input power or output power were determined in Section 3.4.3 and the Graph 6 was plotted based on the results. From the Graph 6, it was obtained that the output power was increased as the input power was increased. The relationship between input power and output power was linearly proportional to each other when the input power was 200 watts onward. Then, the equation in the graph was representing their relationship. The gradient of graph had shown the general efficiency of the inverter which was about 96% when the input power was above 200 watts.

Graph 6: Inverter's Output Power (W) Versus Inverter's Input Power (W)

Another Graph 7 was plotted to see the relationship between inverter's efficiency and output power. From the Graph 7, it was obtained that the efficiency of inverter was not fixed at 96% and it is slowly increased with the output power until it reaches up certain level. The higher efficiency was obtained when the output power was high. The efficiency was below 70% when the output power was below 500 watts and the 96% of efficiency was showed when the output power was above 1500 watts. In other word, the minimum input power for efficiency to be 96% was 1800 watts.

Graph 7: Inverter's Efficiency (%) Versus Inverter's Output Power (W)



The low efficiency at the low input power can be explained as the power were consumed by inverter as power source to power up the internal electronics device, consumed by electronics component during power conversion and some loss in the heat dissipation form.

In the ideal case, the efficiency was 100% where the output power is same as input power as there is no power loss in the inverter. However, in real world there must have some losses. For example, let assumes the power source for inverter was 30 watts which was fixed, 5 watts for heat dissipation and 20 watts for switching loss. Two different input powers of 200 watts and 2000 watts were supplied to the inverter to compare their efficiency. The efficiency was calculated based on the equation 6.1.

$$\begin{aligned}
 \text{Efficiency} &= \frac{\text{Output Power}}{\text{Input Power}} \\
 &= \frac{\text{Input Power} - \text{Power Loss}}{\text{Input Power}}
 \end{aligned}
 \tag{6.1}$$

$$\begin{aligned}
 \text{Efficiency with 200 watts input power} &= \frac{145}{200} \times 100\% \\
 &= 73\%
 \end{aligned}$$

$$\begin{aligned}
 \text{Efficiency with 2000 watts input power} &= \frac{1945}{2000} \times 100\% \\
 &= 97\%
 \end{aligned}$$

The results had proved the efficiency was higher when the input power was high as the ratio of power loss was reduced as the input power was high.

From the Graph 6 and 7, it was obtained that some points or data were strangely plotted in the graph. However, it can be ignored as minor error during data collection as the results were plotted based on four days reading. Therefore, it can focus and analysed on the regions the most points lay on.

Although, the efficiency of inverter was vary with input power but the average efficiency of inverter can be considered as 80% with 20% of power loss in the inverter.

6.5 Efficiency of PV System

From the Chapter 4, the ideally energy generated in a single day was 14.72 kWh and the average energy generated in a single day was 11 kWh as shown in Section 6.2. The average efficiency of the PV system can be calculated based on these values as following.

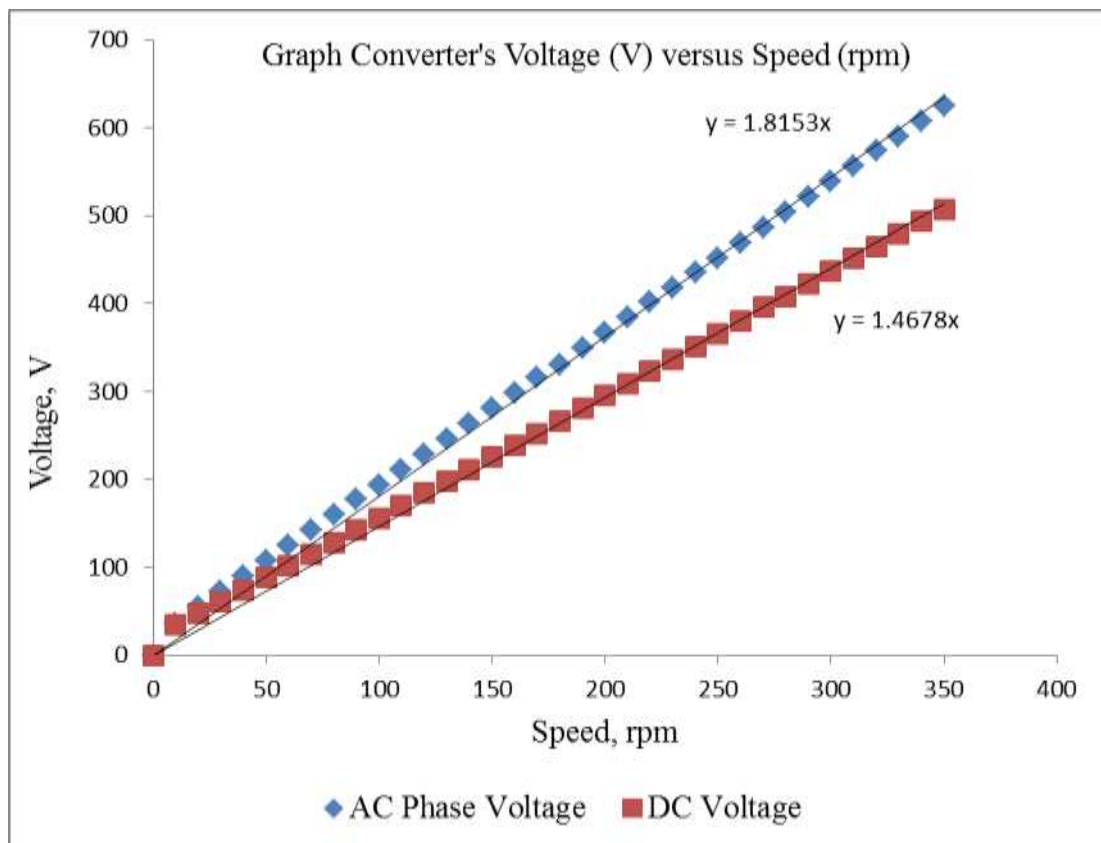
$$\begin{aligned} \text{Average Efficiency} &= \frac{\text{Average energy generated in a day}}{\text{Ideal energy generated in a day}} \times 100\% \\ &= \frac{11}{14.72} \times 100\% = 75\% \end{aligned}$$

Hence, the efficiency of PV system was only about 75% even though the operation hour for real case was more 6 hour than ideal case. The other 25% can be explained as the losses along the PV system or the hours of PV panel receives direct sun shine was less than 4 hour as stated in ideal case. From the Section 6.3 and 6.4, the average power losses in the PV system were 24% which was approximately same as calculated value which had proved the power were losses in the inverter and wires.

6.6 HAWT System

The results from Section 3.5 were recorded and processed in program Microsoft Excel. The graphs were plotted based on these results as shown in Graph 8 and 9. From the graph 8, the voltages of converter were plotted with the wind emulator's speed. It was obtained that the voltage was increased as the speed was increased. The relationship between voltage and speed was linearly proportional to each other. This relationship was further represented by the equation shown in the Graph 8.

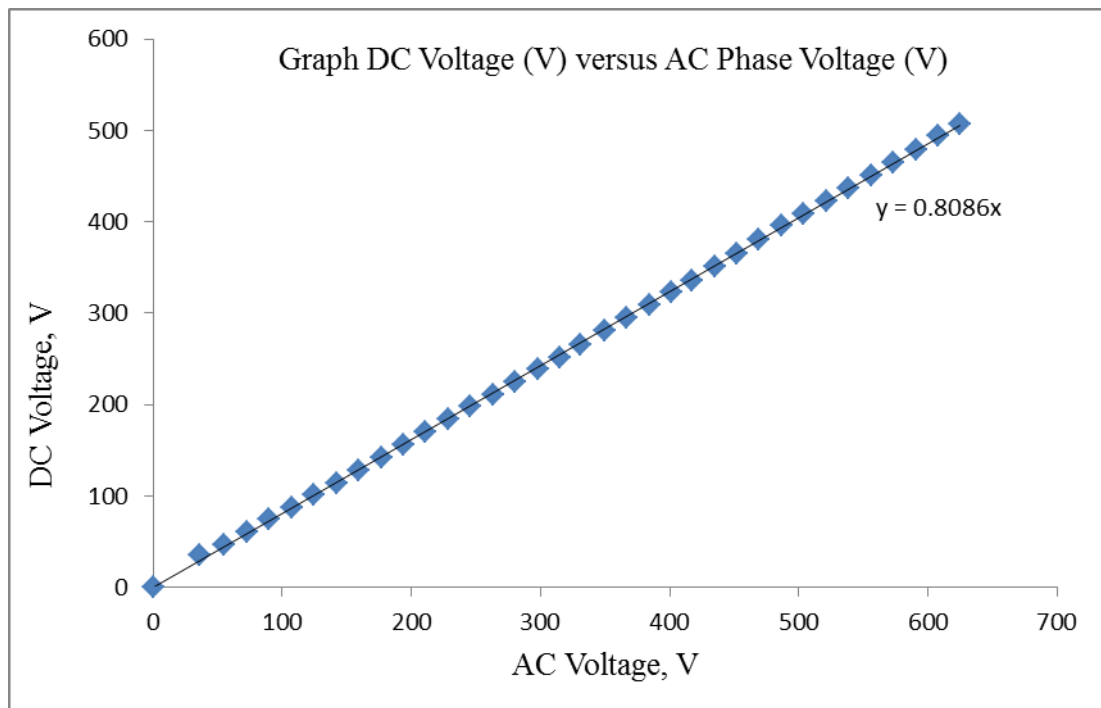
In ideal case, the input voltage and output voltage was same as the efficiency of converter was assumed to be 100%. However, in practical there must have some voltage drop during the conversion so the efficiency was not 100%. This had explained the input voltage was always higher than the output voltage with the same level of speed as shown in the Graph 8.

Graph 8: Converter's Voltage (V) versus Speed (rpm)

Another Graph 9 was plotted to determine the efficiency of converter for voltage. From the Graph 9, the relationship between DC voltage and AC Phase voltage was obtained to be linearly proportional to each other. The efficiency of converter was represented by the gradient of the graph which was 81%.

In general, the efficiency of converter should be expressed in term of power instead of voltage. However, it was unable to feed the HAWT system to the grid system due to the malfunction of inverter in this project. Therefore, it can expressed in voltage term as the circuit was incomplete where no current flow through the system and no power were generated.

Graph 9: Converter's Output DC Voltage (V) versus Input AC Phase Voltage (V)



The objectives to show the wind power output profile and identify the maximum wind turbine power output of the month were failed. The main reason was due to the malfunction of inverter in HAWT system. Besides, the wind stream at the UTAR was not so ideally to allow the operation of wind turbine which means the percentage of wind turbine to rotate in a day was less.

6.7 VAWT Rotor speed

In the Section 3.6.1, the frequency and number of pole for the generator were determined through the DAQ platform. The results was recorded and shown in Table 6.1.

Table 6.1: Results adopted from Section 3.6.1

Industrial Fan		Obtained from LabVIEW		Tachometer	Difference of rotor's speed (%)
No.of fan	Speed	No.of Pole	Speed of rotor (RPM)	Speed of rotor (RPM)	
1	L	8	127	135	5.9
1	M	16	210	208	1.0
1	H	16	248	249	0.4
2	L, L	16	285	285	0
2	L, M	16	323	319	1.3
2	M, M	16	338	342	1.2
2	M, H	16	368	370	0.5
2	H, H	16	398	393	1.3
H – Highest Speed Mode M- Medium Speed Mode L-Lowest Speed Mode					

From the Table 6.1, the number of pole for the generator was 16 poles. The results of speed determined through the DAQ platform was verified by tachometer. The difference between the results speed obtained from DAQ platform and tachometer were less than 1.4 %. This small difference can be explained as the resolutions of sensitive for DAQ platform and tachometer were different. Hence, it had proved that the rotor speed can be determined through the formula with the known values of frequency and number of pole for the generator.

Besides, it had obtained that the speed of rotor was increased as the speed of fan was increased. The fans were used to create the wind stream where the higher fan speed been adjusted, the stronger the wind stream or wind speed created by the fan. Therefore, in the other way the rotor speed was increased as the wind speed was increased.

6.8 Performance of VAWT

6.8.1 Relationship between the wind and rotor speed

The results adopted from Section 3.6.2.1 were summarized in Table 6.2. Although, the specific value of wind speed and volume of speed were unknown but it can be represented by the number of fans and the mode of speed that were applied in Section 3.6.2.1. The relationship between the wind and rotor speed was roughly analysed as the specific value of wind speed and wind volume were unknown. From Table 6.2, it was obtained that the rotor speed was increased as the volume and speed of wind were increased. Therefore, it was proved that the rotor speed was affected by the wind speed and the volume of wind acting on the blades.

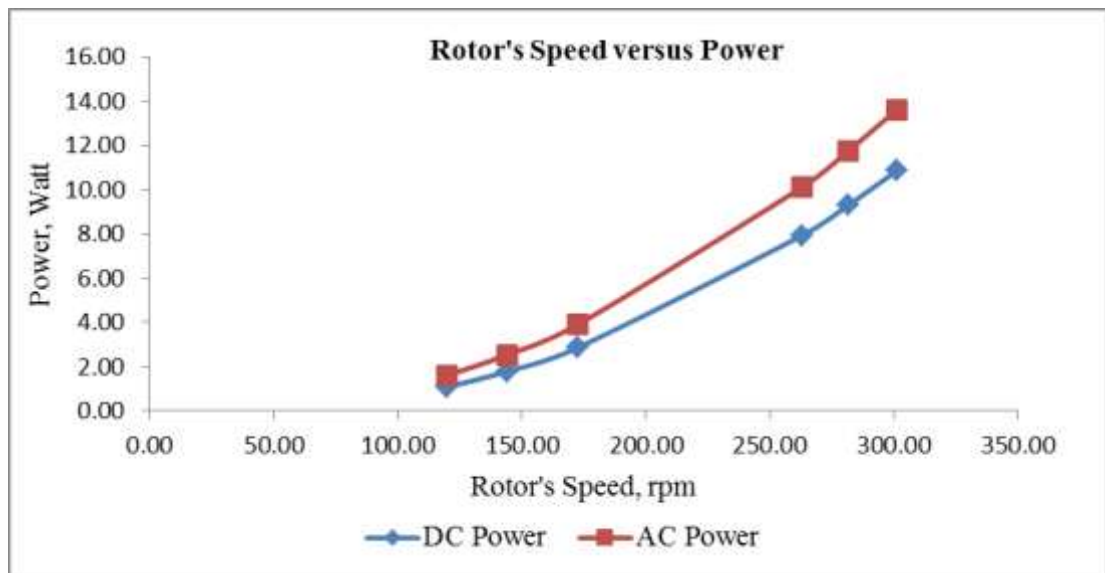
Table 6.2: Fixed Load with Variable Wind Speed

Industrial Fan		Rotor speed,(RPM)	Input AC Power (W)	Output DC Power (W)	Efficiency (%)
No. of fan	Speed				
1	L	120.04	1.61	1.08	67.17
1	M	144.07	2.54	1.79	70.48
1	H	172.31	3.89	2.85	73.20
2	L,L	262.93	10.11	7.93	78.41
2	L,M	281.56	11.75	9.30	79.13
2	L,H	301.14	13.62	10.86	79.74
H – Highest Speed Mode M- Medium Speed Mode L-Lowest Speed Mode					

6.8.2 Relationship between the input power and output power

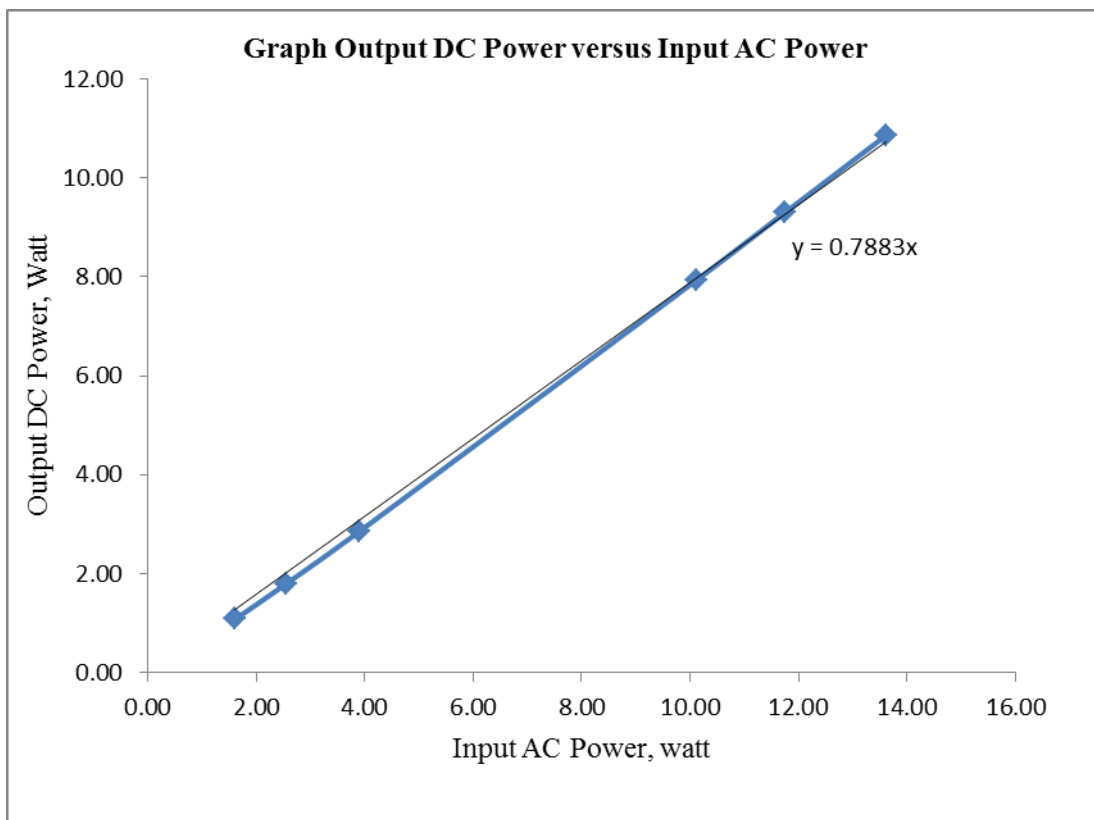
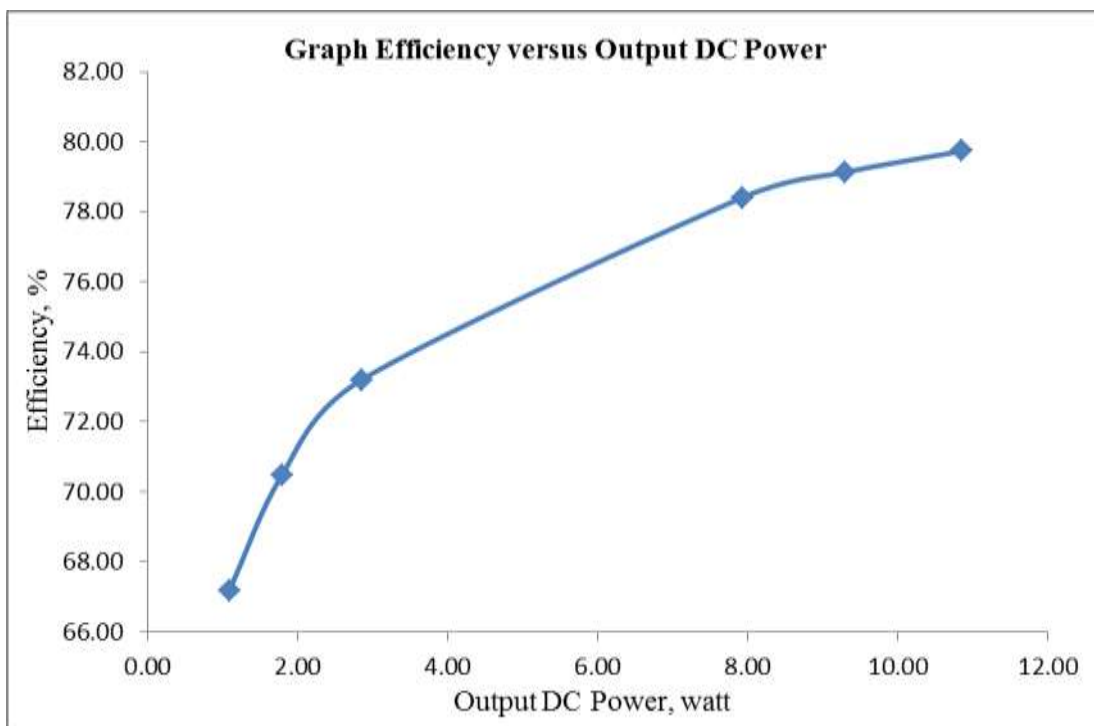
The Graph 10 was plotted based on Table 6.2. From Graph 10, the power was increased as the speed was increased where the load was fixed to be constant load. However, the input power was not the same as output power, which means some power was lost during the conversion process in the rectifier.

Graph 10: Converter's Output DC Voltage (V) versus Input AC Phase Voltage (V)



The power losses in the converter can be explained as the voltage drop along the diode as there were diodes in the converter to do the conversion and some were lost as heat. The Graph 11 had shown the relationship between the input power and the output power. The relationship between them was linearly proportional to each other and it was represented by the equation as shown in the Graph 11.

From the Graph 12, the efficiency of the converter was varying with the output power. However, the efficiency was increased as the output power was increased. The efficiency was below 70% when the input power was around 3 watts. Therefore, the power loss should be reduced in order to improve the efficiency of converter.

Graph 11: Converter's Output DC Power (W) versus Input AC Power (W)**Graph 12: Converter's Efficiency (%) versus Output DC Power (W)**

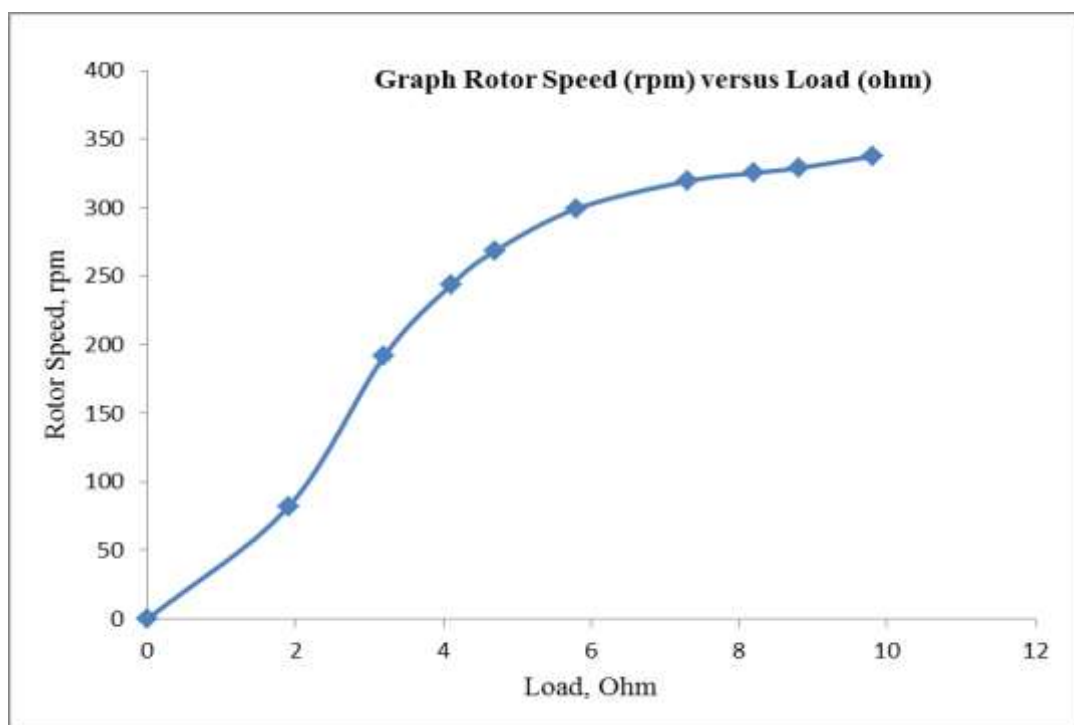
6.8.3 Relationship between rotor Speed and load

The results adopted from the Section 3.6.2.2 were summarized in the table 6.3. The Graph 13 was plotted under this section to analyse the relationship between rotor speed and load applied.

Table 6.3: Fixed Wind Speed with Variable Load

No .	Load, ohm	Rotor Speed, rpm	Current (A)		Voltage (V)		Power (W)		Efficiency (%)
			AC	DC	AC	DC	Input AC	Output DC	
1	0	0	0	0	0	0	0	0	0.00
2	1.90	81.62	0.55	0.71	2.23	1.30	2.11	0.92	43.37
3	3.20	191.87	1.16	1.42	5.30	5.20	10.60	7.40	69.78
4	4.10	243.42	1.36	1.66	6.75	7.08	15.91	11.76	73.95
5	4.70	268.56	1.42	1.73	7.47	8.02	18.33	13.87	75.69
6	5.80	299.30	1.40	1.70	8.37	9.25	20.35	15.73	77.31
7	7.30	319.34	1.23	1.48	9.01	10.17	19.14	15.04	78.58
8	8.20	325.32	1.10	1.31	9.22	10.50	17.50	13.81	78.90
9	8.80	328.95	1.01	1.23	9.37	10.69	16.35	13.17	80.54
10	9.80	337.57	0.93	1.14	9.66	11.09	15.56	12.62	81.13

Graph 13: Rotor speed (rpm) versus Load (ohm)

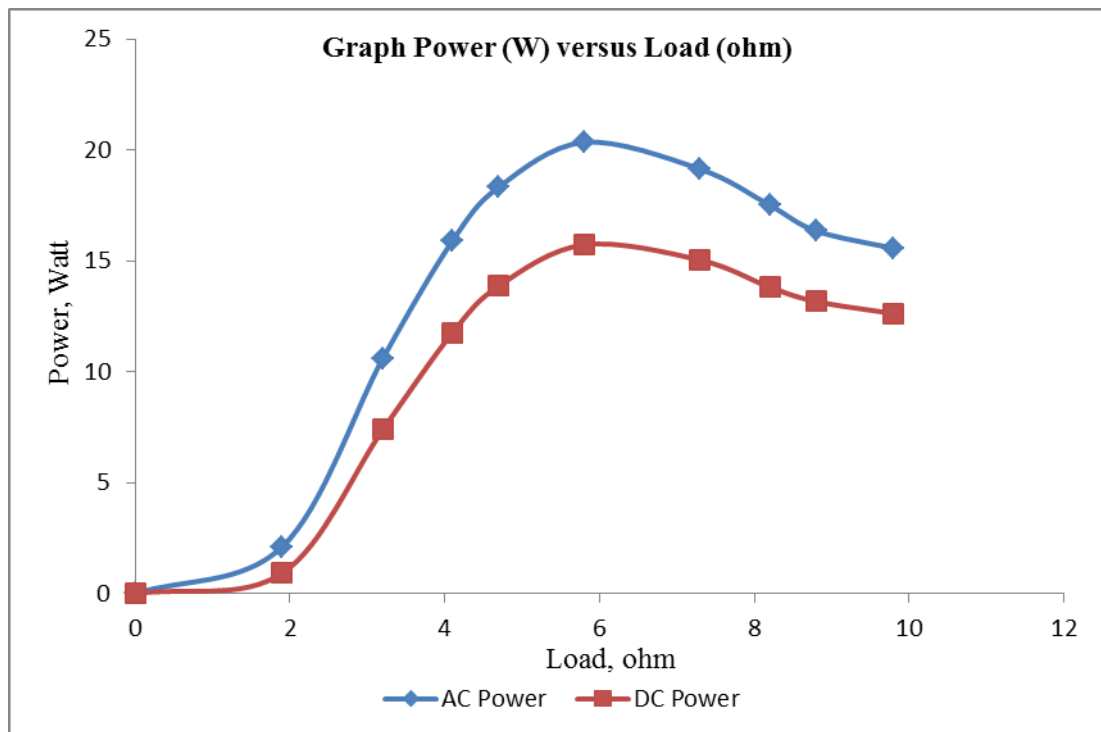


From the Graph 13, it had obtained that the rotor speed was increased as the load was increased where the level of wind speed was fixed to be constant. Hence, the rotor speed was affected by the amount of load applied to the circuit.

6.8.4 Relationship between Output Power and load

The Graph 14 was plotted based on the result from Table 6.3. From the Graph 14, the power generated by the VAWT was increased as the load was increased until 5.8 ohm of load. In the Table 6.3, it had obtained that the rotor speed was increasing with the load. The graph was explained as written in next paragraph.

Graph 14: Power (W) versus Load (ohm)



From the equation 2.3, the generator's output power was related to torque and speed of the generator. In order to generate more power, the speed and torque of generator must be increased. Meantime, the torque was related to the current where more current were produced when there were more torque. From the Graph 14, the

maximum power produced by the generator at this fixed level of wind speed and volume was 20.35 watts. However, the inertia of blades had kept the rotor speed continues raises. This had caused the output power been reduced as the torque was reduced to keep the acceleration of generator. As torque was proportional to the current, the current was followed been reduced as shown in table 5.0. All of these had leaded the output power to be less although the rotor speed was increased.

6.9 Overall Results

The results showed in the above were not complete version. The reason was due to the original results were too many and it may not necessary to display all the value in the report. However, almost all the results were arranged in the Microsoft Excel file and named according to the section name. Hereby, the full version or original versions of the results were attached inside the softcopy CD-ROM according to the section name for reference.

CHAPTER 7

CONCLUSIONS AND RECOMMENDATIONS

7.1 Conclusions

As a conclusion, the project is considered quite successful as it had been done within the period. Although, some objectives such as determining the output profile and maximum power of the month for the HAWT system were failed to achieve. However, these objectives can be determined once the new inverter is replaced as the platform was already built and tested with PV system as shown in Chapter 3.

By doing this project, it was understood that the both output power from PV and WT systems were strongly dependent or affected by the factor of natural energy. However, the PV system was much more reliable compared to the WT system as the potential of solar energy was much more reliable than wind energy in UTAR campus. The results had shown the average efficiency of the PV system was 75 % and the total energy produced in a month was 324.63 kWh.

Besides, the mechanism of the WT system was much more complicated compared to the PV system. The PV system only requires one inverter at the output while the WT system requires a converter and an inverter. It was understood that there was always a power loss during the power conversion. Hence, the efficiency of the WT system was eventually much lower than the PV system as much power was lost during the power conversion process.

7.2 Recommendations

The power output of PV system can be improved by replaces the present PV panel's structure into a structure that can move according to the position of sun shine. This can helps to increase the percentage of direct sun shine to the PV panels and improve the output power. Besides, the heat ventilation system can be involves into PV system to reduce the temperature of solar cell. This is because the performance of solar cell is reducing when the temperature is increasing.

Based on the Chapter 6, none of the results were adopted based on the natural wind as the potential of wind stream at the UTAR campus was not ideally to suit wind turbine. The suggestion to improve the wind turbine system are increases the potential of wind stream acts on the blade by relocates the wind turbine at much open area and much higher place at the UTAR campus.

REFERENCES

- Ahmad, H., 2012. *Wind turbine technology*. 1st ed. Delmar cengage learning.
- Bracken, M., 2011. *Centurion energy*, [Blog] 07 March. Available at: <http://centurionenergy.net/index.php> [Accessed 1 August 2012].
- Concinnity Solar, 2013. *Brighter solution for a greener world*. [Online]. Available at: <http://concinnitysolar.com> [Accessed 20 March 2013].
- General Microgrids, 2012. *General Microgrids Balance Energy*. [Online]. Available at: <http://www.generalmicrogrids.com> [Accessed 23 August 2012]
- Leong, H. Y., 2011. *Need for more power plants, rising power demand seen*. The Star Online, [Online]. Available at: <http://biz.thestar.com.my/news/story.asp?file=/2011/7/1/business/9009124&sec=business> [Accessed 19 August 2012].
- Ministry of Energy, Green Technology and Water, 2011. *Launching date for the implementation of feed-in tariff system*. [Online]. Available at: <http://www.kettha.gov.my/en/content/minister-energy-green-technology-and-water-announces-revised-launching-date-implementation-f> [Accessed 20 August 2012].
- Ministry of Science, Technology and Innovation (MOSTI), 2011. *General climate of Malaysia*. [Online]. Available at: http://www.met.gov.my/index.php?option=com_content&task=view&id=75&Itemid=1089&limit=1&limitstart=0 [Accessed 23 August 2012]

Mukund, R. P., 2006. *Wind and solar power systems design, analysis and operation*. 2nd ed. New York: Talyor and Francis.

Pramod, J., 2011. *Wind energy engineering*. 1st ed. McGraw-Hill Professional

Remus, T., Marco, L., and Pedro R., 2011. *Grid converters for photovoltaic and wind power systems*. John Wiley and Sons.Ltd.

TES Electrical Electronic CORP, 2008. *Power Analyzer User Manual*. Taiwan: TES.

TIMAR Technology Co.,Ltd. *CXF-400W User Manual*. China: TIMAR

APPENDICES

APPENDIX A: Gantt chart (Semester 1)

Activities	Week														
	1	2	3	4	5	6	7	8	9	10	11	12	13	14	15
FYP Title Selection															
Meet Supervisor															
PV Research and Study															
PV Investigation and Testing															
Design Platform															
PV Data Collection															
Prepare Progress Report															
Presentation															

APPENDIX C: PV Inverter Datasheet A

SINGLE PHASE INVERTERS

SUNZET TL

Single-phase on-grid solar inverters range

Description



The SUNZET TL combines design and versatility with ease of operation. An outstanding feature of SUNZET TL inverters is their 96% efficiency without transformer.

The SUNZET TL stands out because of its RS-485 communications with the centralised supervision and control system and all its parameters can be configured locally (optional).

The SUNZET TL offers a range of input DC voltages of between 120-500 vdc and IP65 watertightness.



Sunzet 5 TL

Features

- > Range of input voltages (120-500 VDC)
- > Maximum power point tracking (MPPT)
- > High energy efficiency, higher than 96%
- > Very low harmonic distortion, THD < 4%
- > Direct mains connection
- > Unlimited parallel connection arrangements
- > Anti-islanding protection with automatic shut down
- > Monitoring from the unit with LCD
- > Protection against: inverse polarity, short-circuits, overvoltages, isolation failure
- > RS-485 communication port (optional)
- > Compact size, light weight
- > Remote SCADA (SWS 200): communications system, parameter display, inverter records control, production data storage etc. (optional)

APPENDIX D: PV Inverter Datasheet B

ELECTRICAL CHARACTERISTICS					
Model	Sunzet TL 2	Sunzet TL 3	Sunzet TL 3,6	Sunzet TL 4	Sunzet TL 5
Reference	20104	20105	20106	20107	20108
Max. output power	2 KW	3 KW	3.6 KW	4 KW	5 KW
SYSTEM					
Conversion mode	High frequency PWM				
Electromechanical method	Low loss transformer (optional)				
DC INPUT					
Nominal DC voltage	360V				
Maximum DC voltage	500V				
Operating range DC	120-500V				
Operating range DC for MPPT	150-450V				
No. input circuits	1(14.6A Max. x circuit)	1(22A Max. x circuit)	2(12.2A Max. x circuit)	2(14A Max. x circuit)	2(17.65A Max. x circuit)
AC OUTPUT					
No. phases/No. wires	1- phase/2- wires or 1 - phase/ 3 - wires (LNG)				
Nominal voltage AC	230V				
Nominal frequency	50/60 Hz				
Nominal output current AC	8.7 A	13 A	15.2 A	17.4 A	21.7 A
Power factor	Over 0.99 (at nominal output current)				
European efficiency	98%				
PROTECTION					
Input	Ground fault / DC isolation fault				
Output	Over-undervoltage/ Over-under frequency / Islanding				
Protection class	IP 65				
Anti-islanding detection	Active method: reactive power control				
INTERFACE					
Standard	RS232				
Optional	RS485				
ENVIRONMENTAL CHARACTERISTICS					
Temperature	-10°C to +50°C				
Relative humidity	0-90% without condensation				
Altitude	< 2000m				
MECHANICAL CHARACTERISTICS					
Dimensions (WxHxD) mm	170x455x430		170x445x510		
Weight kg	22		29		
Cooling	Free convection				
STANDARDS					
Certificates	CE Marking, UL, VDE				
Directives	73/23/CEE-93/68/CEE 2004/108/CEE				
Standards	EN50178 EN 61000-6-2, EN 61000-6-3, EN 61000-3-2, EN 61000-3-3 IEC60148				
Countries standards					
USA	UL1741, IEEE1547 FCC				
Italy	ENEL				
Germany	VDE0126-1-1				
Australia	AS/NZS3100:2009, AS/NZS4777.2:2005 AS/NZS4477.3:2005				

Power derating protection at low DC input & high room temperature.
These specifications may be changed without notice.

APPENDIX E: NI 9225 Specification A

Product Name	NI 9225 Measurement Bundle
Product Family	Industrial I/O
Form Factor	Wireless , CompactDAQ , Ethernet , USB
Part Number	000000-00
Operating System/Target	Real-Time
LabVIEW RT Support	Yes
Measurement Type	Voltage
RoHS Compliant	Yes
Signal Conditioning	Anti-aliasing filter
Analog Input	
Channels	3 , 0
Single-Ended Channels	0
Differential Channels	3
Resolution	24 bits
Sample Rate	50000 S/s
Bandwidth	24.56 kHz
Max Voltage	300 V
Maximum Voltage Range	-300 V , 300 V
Maximum Voltage Range Accuracy	0.034 V
Simultaneous Sampling	Yes
Input Impedance	1 MOhm
Analog Output	
Channels	0
Digital I/O	
Bidirectional Channels	0
Input-Only Channels	0
Output-Only Channels	0
Number of Channels	0
Counter/Timers	
Counters	0
Physical Specifications	

APPENDIX F: NI 9225 Specification B

Length	9 cm
Width	9 cm
Height	2.3 cm
I/O Connector	MINI-COMBICON, 3.5 mm (2-Position)
Minimum Operating Temperature	-40 °C
Maximum Operating Temperature	70 °C
Minimum Storage Temperature	-40 °C
Maximum Storage Temperature	85 °C

APPENDIX G: NI 9227 Specification A

Specifications Summary	
General	
Product Name	NI 9227 Measurement Bundle
Product Family	Industrial I/O
Form Factor	Ethernet , USB , Wireless , CompactDAQ
Part Number	000000-00
Operating System/Target	Real-Time , Windows
Measurement Type	Current
RoHS Compliant	Yes
Termination Type	Screw-Termination
Signal Conditioning	Anti-aliasing filter
Analog Input	
Channels	4 , 0
Single-Ended Channels	0
Differential Channels	4
Resolution	24 bits
Sample Rate	50 kS/s
Bandwidth	24.6 kHz
Maximum Current Range	-5 Arms , 5 Arms
Maximum Current Range Accuracy	0.011 mA
Simultaneous Sampling	Yes
Input Impedance	12 mOhm
Analog Output	
Channels	0
Digital I/O	
Bidirectional Channels	0
Input-Only Channels	0
Output-Only Channels	0
Number of Channels	0

APPENDIX H: NI 9227 Specification B

Counter/Timers	
Counters	0
Physical Specifications	
Length	9 cm
Width	2.3 cm
I/O Connector	Screw terminals
Minimum Operating Temperature	-40 °C
Maximum Operating Temperature	70 °C
Minimum Storage Temperature	-40 °C
Maximum Storage Temperature	85 °C
Timing/Triggering/Synchronization	
Triggers cDAQ Chassis	No

APPENDIX I: NI cDAQ-9174 Specification A

Specifications	
Specifications Documents	
Specifications	
Data Sheet	
Specifications Summary	
General	
Product Name	cDAQ-9174
Form Factor	CompactDAQ
Product Type	Chassis
Part Number	781157-01
Operating System/Target	Windows
LabVIEW RT Support	No
Operating Relative Humidity	10 percent , 90 percent
Chassis	
Number of Slots	4
Total Available Power	15 W
Input Voltage Range	9 V , 30 V
Built-In Trigger	No
Counter/Timers	
Counters	4
Resolution	32 bits
Bus Interface	
USB Specification	USB 2.0 Hi-Speed
High-Performance Data Streams	7
Types Available	Digital Output , Counter/Timer Input , Digital Input , Analog Output , Analog Input
Shock and Vibration	
Operational Shock	30 g
Random Operating Frequency Range	5 Hz , 500 Hz
Random Vibration	0.3 g

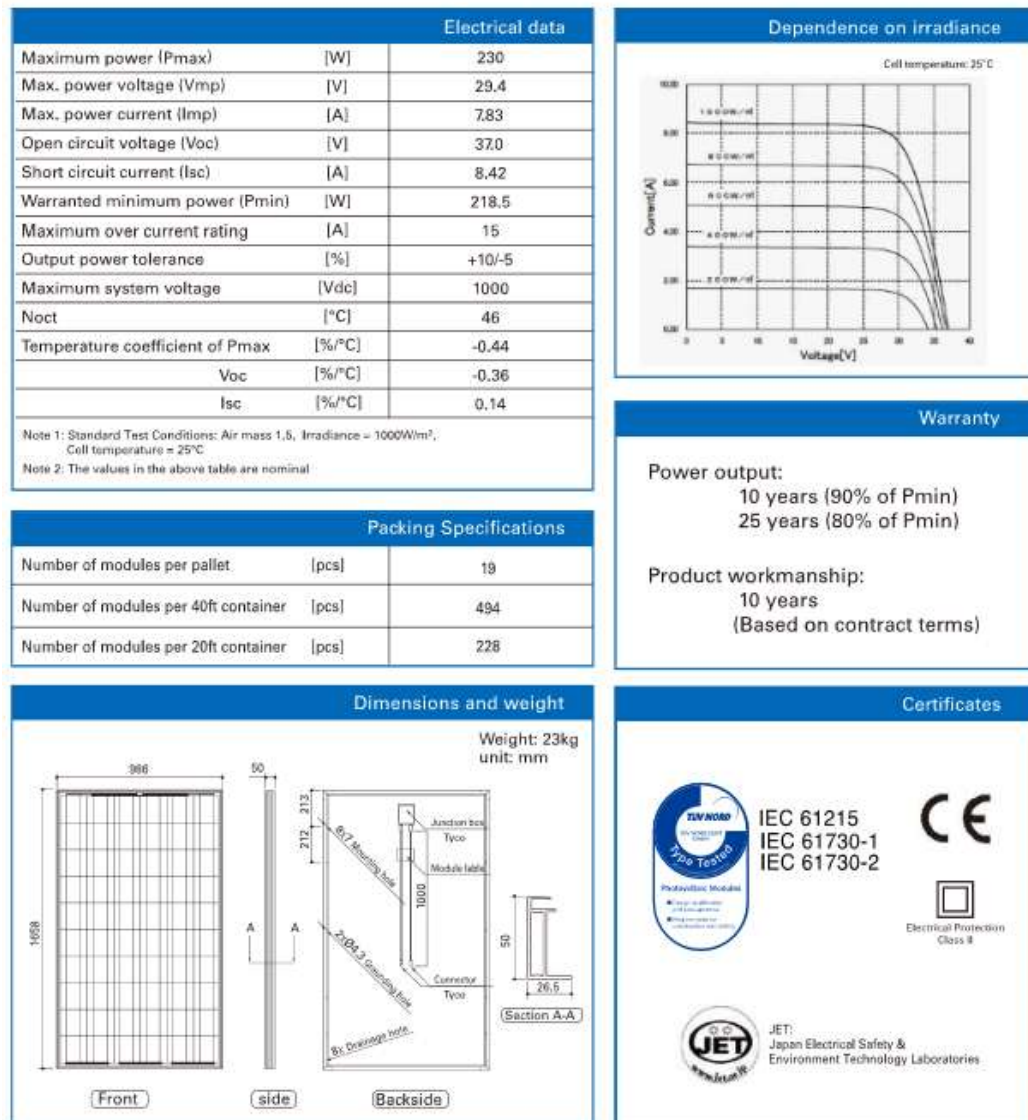
APPENDIX J: NI cDAQ-9174 Specification B

Physical Specifications	
Length	15.9 cm
Width	8.81 cm
Height	5.89 cm
Weight	574 gram
Minimum Operating Temperature	-20 °C
Maximum Operating Temperature	55 °C
Maximum Altitude	5000 m

APPENDIX K: Photovoltaic Module Specification

Electrical and Mechanical Characteristics

VBMS230AE01



CAUTION! Please read the operating instructions carefully before using the products.

Due to our policy of continual improvement the products covered by this brochure may be changed without notice.

Panasonic Asia Pacific Pte. Ltd.

Panasonic Eco Solutions Asia Pacific

- 101 Thomson Road, #75-03/05, United Square,
Singapore 307591
- Tel: +65-6255-5473
- Fax: +65-6253-5689

Panasonic

All Rights Reserved © 2012 COPYRIGHT SANYO Electric Co., Ltd.
 Specifications are subject to change without notice.
 03/2012

APPENDIX L: HAWT Specification

ELECTRICAL CHARACTERISTICS				
Model	LET 300	LET 600	LET 2000	LET 6000
References				
Voltage	LET 300	LET 600	LET 2000	LET 6000
12 V	20130	-	-	-
24 V	20131	20132	20136	-
48 V	-	20133	20137	-
On-grid	-	-	20139	-
Rotor Type	3-Blade upwind		3-Blade downwind	
Blade Material	Glass Reinforced Nylon		Glass Reinforced Composite	
Rated Output	85watts @ 8m/s (18mph)	160 watts @ 7.2m/s (16.2mph)	1100watts @ 8m/s (17mph)	5000watts @ 11m/s (24mph)
Peak Output	300 watts	700 watts	2500 watts	6000 watts
Cut-in speed	3m/s (6.7mph)			
Estimated AEP (per year) Depending on site location & wind	250-400kWh	250-1900kWh	2000-4500kWh	7000-20,000kWh
Generator Type	3-Phase Brushless NIB rotor PMA		3-Phase Brushless NIB dual rotor PMA	
Off-grid output voltage	12 or 24V	24 or 48V	24V or 48V	
On-grid output voltage	-	-	300V DC Grid tie	
GENERAL FEATURES				
Lifetime & Servicing	20 years. Annual inspection recommended			
Warranty	2 years			
Control system	-	-	Flight Computer, Auto Shut-down Over Voltage	Flight Computer, Auto Shut-down Over Voltage, Mechanical Brake
Grid-Tie Equipment:	Windzet inverter of Zigor			
ENVIRONMENTAL AND MECHANICAL FEATURES				
Weight	6.5 Kg	19.5Kg	60kg (head)	265kg (head)
Rotor Diameter	1 metre	1.54 metres	3 metres	6.0 metres
Acoustic level	-	-	53dB(A)	
ACCESSORIES				
Model	LET 300	LET 600	LET 2000	LET 6000
	Guyed tower kit	Guyed tower kit	Free Standing Tower Hydraulic Lift Arm Frame Windzet inverter SP 2 KW	-

APPENDIX M: VAWT Specification A



Eco-Smart, Inc.

TOLL FREE: (888)329-2705 FAX: (941)377-9460 info@eco-smart.com

Vertical Axis Wind Turbine System

WE-CXF-400 WE-CXF-600 WE-CXF-1000 WE-CXF-2000 WE-CXF-3000

Concept

A COMBINATION OF TWO BLADES

- **Darrieus Blade rotates at high efficiency:** Chosen from specifications in aircraft blade data bases and optimized by Computational Fluid Dynamics systems, the Darrieus Blade is 10% to 20% more efficient than comparably sized Darrieus blades.
- **Savonius Blade rotates at high torsion:** Optimized by Computational Fluid Dynamics systems, with a re-designed radian shape that reduces noise and vibration.

ALTERNATOR

Direct-drive permanent-magnet synchronous generator is integrated precisely with the blades. This design requires less starting torque, improves efficiency and lowers cost by eliminating the need for a gear box.

ELECTRICAL CONTROL

- **Maximum Point Power Tracking**
- **Advanced computer cooling system** enhances performance and prolongs the life of the machine.
- **Full function anti-storm mode** operates in strong wind and can be customized to local weather.



Features

- Can generate up to 50% more electricity per year than conventional turbines with the same swept area.
- No need to “right themselves” into the wind.
- Unique damper design overcomes noise and vibration.
- All aluminum-alloy construction:
 - ~ Lighter weight, easier to install.
 - ~ More strength and power.
 - ~ Better generator cooling.
 - ~ Improved electromagnetic shielding.
 - ~ All components are recycleable.

APPENDIX N: VAWT Specification B

Vertical Axis Wind Turbine System

WE-CXF-400 WE-CXF-600 WE-CXF-1000 WE-CXF-2000 WE-CXF-3000

Specifications

Rated Power	Output Voltage	Output Current	Diameter	Height	Weight
400W	24V	<20 Amps	49.6" 1240MM	44.8" 1120MM	29KG
600W	24V	<20 Amps	60" 1500MM	52.8" 1320MM	40KG
1000W	48V	<50 Amps	96" 2400MM	93.6" 2340MM	188KG
2000W	48V	<80 Amps	132" 3300MM	129.6" 3240MM	329KG
3000W	48V	<130 Amps	144" 3600MM	141.2" 3630MM	419 KG

Start-up Wind Speed:	1m/s	Rated Power Wind Speed:	12m/s
Survive Wind Speed:	60m/s	Cut-out Wind Speed:	15m/s
Blades:	Aluminum Alloy		
Generator:	3 phase AC, permanent magnet		
Braking system:	3 phase short-circuit by NFB braking		



APPENDIX O: Current Transducer Specification A

Solid State Sensors

Linear Current Sensors

CS Series

**FEATURES**

- Linear output
- AC or DC current sensing
- Through-hole design
- Fast response time
- Output voltage isolation from input
- Minimum energy dissipation
- Maximum current limited only by conductor size
- Adjustable performance and built-in temperature compensation assures reliable operation
- Accurate, low cost sensing
- Operating temperature range -25 to 85°C
- Housing: PET polyester

LINEAR CURRENT SENSORS

MICRO SWITCH CS series linear current sensors incorporate our 91SS12-2 and SS94A1 linear output Hall effect transducer (LOHET™). The sensing element is assembled in a printed circuit board mountable housing. This housing is available in four configuration as shown in mounting dimension figures 1, 1a, 2 and 2a. Normal mounting is with 0.375 inch long 4-40 screw and square nut (not provided) inserted in the housing or a 6-20 self-tapping screw. The combination of the sensor, flux collector, and housing comprises the holder assembly. These sensors are ratiometric.

ORDER GUIDE — BOTTOM MOUNT WITH 9SS SENSOR, SOURCE OUTPUT

Catalog Listing	Mtg. Dim. Fig.	Supply Volt. (Volts DC)	Supply Current (mA Max.)	Sensed Current (Amps Peak)	Offset Volt. (Volts ±10%)	Sensitivity mV-N* At 12 VDC		Offset Shift (%/°C)	Response Time (μ Sec.)
						Nominal	± TOL		
CSLA1CD	1	8 to 16	19	57	Vcc/2	49.6	5.8	±.05	3
CSLA1CE	1	8 to 16	19	75	Vcc/2	39.4	4.4	±.05	3
CSLA1DE	2	8 to 16	19	75	Vcc/2	39.1	4.8	±.05	3
CSLA1CF	1	8 to 16	19	100	Vcc/2	29.7	2.7	±.05	3
CSLA1DG	2	8 to 16	19	120	Vcc/2	24.6	2.1	±.05	3
CSLA1CH	1	8 to 16	19	150	Vcc/2	19.6	1.8	±.05	3
CSLA1DJ	2	8 to 16	19	225	Vcc/2	13.2	1.2	±.05	3
CSLA1EJ	1a	8 to 16	19	225	Vcc/2	13.2	1.5	±.05	3
CSLA1DK	2	8 to 16	19	325	Vcc/2	9.1	1.7	±.05	3
CSLA1EK	1a	8 to 16	19	325	Vcc/2	9.4	1.3	±.05	3
CSLA1EL	1a	8 to 16	19	625	Vcc/2	5.6	1.3	±.05	3

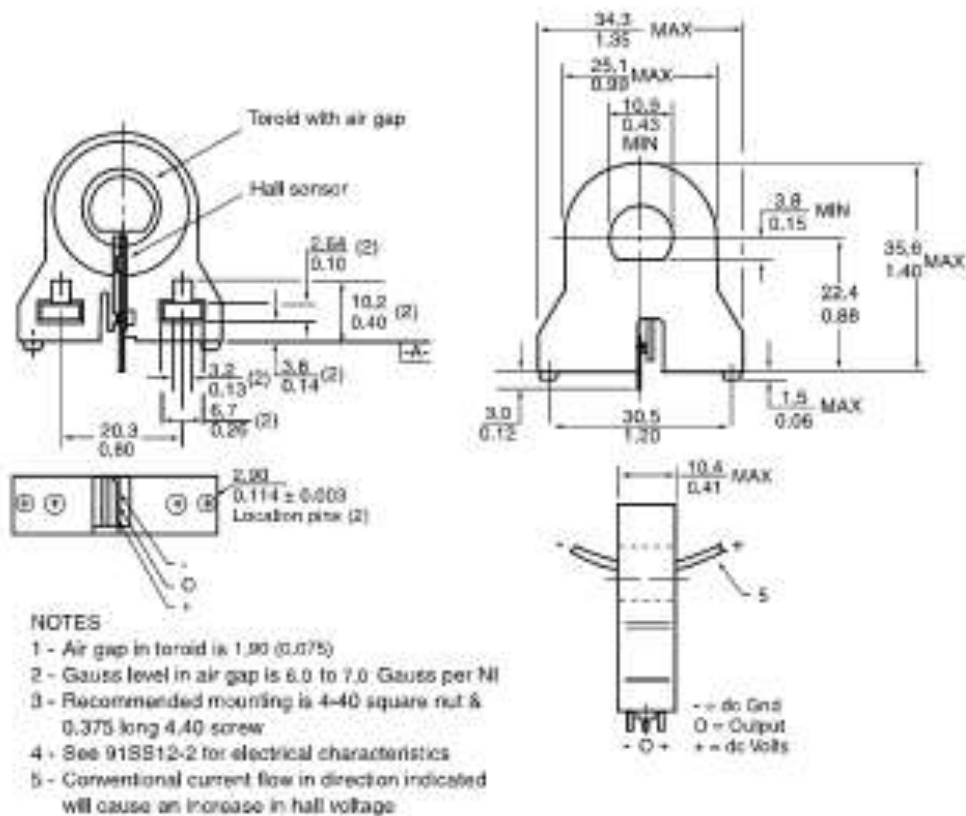
BOTTOM MOUNT WITH SS9 SENSOR, SINK/SOURCE OUTPUT

Catalog Listing	Mtg. Dim. Fig.	Supply Volt. (Volts DC)	Supply Current (mA Max.)	Sensed Current (Amps Peak)	Offset Volt. (Volts ±2%)	Sensitivity mV-N* At 8 VDC		Offset Shift (%/°C)	Response Time (μ Sec.)
						Nominal	± TOL		
CSLA2CD	1	6 to 12	20	72	Vcc/2	32.7	3.0	±.02	3
CSLA2CE	1	6 to 12	20	92	Vcc/2	26.1	2.1	±.02	3
CSLA2DE	2	6 to 12	20	92	Vcc/2	25.6	2.2	±.02	3
CSLA2CF	1	6 to 12	20	125	Vcc/2	19.6	1.3	±.02	3
CSLA2DG	2	6 to 12	20	150	Vcc/2	16.2	1.1	±.02	3
CSLA2DJ	2	6 to 12	20	225	Vcc/2	8.7	0.6	±.02	3
CSLA2DH	2	6 to 12	20	235	Vcc/2	9.8	1.1	±.0125	3
CSLA2EJ	1a	6 to 12	20	310	Vcc/2	7.6	0.7	±.0125	3
CSLA2DK	2	6 to 12	20	400	Vcc/2	5.8	0.5	±.0125	3
CSLA2EL	1a	6 to 12	20	550	Vcc/2	4.3	0.4	±.0125	3
CSLA2EM	1a	6 to 12	20	765	Vcc/2	3.1	0.3	±.007	3
CSLA2EN	1a	6 to 12	20	950	Vcc/2	2.3	0.2	±.007	3

NOTE: When monitoring purely AC current with zero DC component, a capacitor can be inserted in series with the output of the current sensor. The capacitor will block out the effect of the temperature variation of the offset voltage which increases the accuracy of the device.

*N = number of turns

APPENDIX P: Current Transducer Specification B

PCB bottom mount

SENSED CURRENT RANGE	SUPPLY VOLTAGE	REFERENCE
0 to 57 A	6 to 16 Vdc	CSLA1CD
0 to 72 A	6 to 12 Vdc	CSLA2CD
0 to 100 A	6 to 16 Vdc	CSLA1CF
0 to 150 A	6 to 16 Vdc	CSLA1CH